International Journal of Solids and Structures 48 (2011) 2218–2237

Contents lists available at ScienceDirect

International Journal of Solids and Structures

journal homepage: www.elsevier.com/locate/ijsolstr

Non-linear thermo-mechanical behaviour of delaminated curved sandwich panels with a compliant core

Yeoshua Frostig [a,*], O.T. Thomsen [b]

[a] Ashtrom Engineering Company, Chair in Civil Engineering, Technion, Israel Institute of Technology, Faculty of Civil and Environmental Engineering, Haifa 32000, Israel
[b] Department of Mechanical and Manufacturing Engineering, Aalborg University, Aalborg, Denmark

ARTICLE INFO

Article history:
Received 21 May 2010
Received in revised form 2 February 2011
Available online 2 April 2011

Keywords:
Delamination
Curved sandwich panel
Compliant core
High-order
Geometrical non-linear
Energy release rate
Thermal effects
Thermo-mechanical response
Temperature-dependent mechanical properties

ABSTRACT

A non-linear analysis of a delaminated curved sandwich panel with a compliant core, and a delamination (debond) at one of the face–core interfaces, and subjected to a thermal field and a mechanical loading or combined is presented. The mathematical formulation outlines the governing equations along with the stress and displacements fields for the cases where the core properties are either temperature independent (*TI*) or temperature dependent (*TD*). A variational formulation is used following the principles of the high-order sandwich panel theory (HSAPT) to derive the field equations along with the appropriate continuity conditions. The non-linear analysis includes geometrical non-linearities in the face sheets caused by rotation of the face cross sections, and high-order effects that are the result of the radially (transversely) flexible (or compliant) core. The core stress and displacements fields with temperature-dependent (*TD*) mechanical properties are determined in closed form using an equivalent polynomial description of the varying properties. The numerical study describes the non-linear response of delaminated curved sandwich panels subjected to mechanical concentrated loads, thermally induced deformations and simultaneous thermal and mechanical loads. In the combined loading case the mechanical loads are below the limit point load level of the mechanical response, and the imposed temperature field is varied. The results are displayed in terms of plots of various structural quantities along the sandwich panel length (circumference), equilibrium curves and strain energy release rate curves. It is shown that the combined thermo-mechanical response shifts the linear or non-linear responses,observed for the separate cases of either temperature induced deformations or mechanical loading, into a strongly non-linear response with limit point behaviour and large stresses in vicinity of supports, loads and tips of delaminated zone.

1. Introduction

Lightweight curved sandwich structures are being used increasingly in the aerospace, naval and transportations industries due to their excellent stiffness-to-weight and strength-to-weight ratios. Such sandwich structures may contain different types of defects, that can be induced either in the manufacturing process or inflicted during service life due to e.g. impact or fatigue damages. The most detrimental form of defects appears in the form of debonds (delamination) at one of the face-core interfaces, or at both face-core interfaces in more extreme cases. Typical modern sandwich panels are often composed of a low stiffness/strength core material made of polymeric foam or a nomex honeycomb that is flexible in the thickness direction, and laminated composite or metallic face sheets. The core usually provides the shear resistance/stiffness to the sandwich structure, as well as a transverse (through-thickness) support to the face sheets that is associated with core radial normal stresses. The face sheets resist the bending moments and the in-plane loads (in the form of a couple) through their composite action. It should be noted that an imperfection in the form of a debond jeopardizes the composite action of the layered sandwich panel, and thereby cause the face sheets to behave as isolated panels without any mechanical interaction within the debonded region. Traditionally, the design process of sandwich structures examines the responses due to the thermal loading, i.e. the deformations induced by thermal sources and the mechanical loads separately. However, the interaction between the mechanical and thermal loads may lead to an unsafe response with loss of stability and structural integrity, especially when the deformations are large and the mechanical properties (e.g. stiffness and strength) degrade as the temperature level is raised. The thermal degradation of mechanical properties is especially pronounced for polymer foam core materials, where significant degradation of the mechanical properties can occur well within the operational temperature range. For example, PVC foams (Divinycell® and Airex®) lose all stiffness and strength at about 80–100 °C, while PMI foams (Polymethacrylimide, e.g. Rohacell®) lose the heat distortion resistance

* Corresponding author. Tel.: +972 48293046; fax: +972 48295697.
E-mail address: cvrfros@techunix.technion.ac.il (Y. Frostig).

0020-7683/$ - see front matter © 2011 Elsevier Ltd. All rights reserved.
doi:10.1016/j.ijsolstr.2011.03.027

at about 200 °C. Moreover, significant degradation of the properties of the foam occurs at much lower temperatures than the temperatures where a complete loss of stiffness and strength is experienced. Hence, it is clear that a reliable non-linear high-order computational model for curved sandwich panels, that takes into account the localized and the overall responses due to debond imperfections, as well as the interaction between the thermal and mechanical loadings, is required to gain a further understanding of the complex mechanisms and interactions involved. The proposition and development of such a model, based on the non-linear high-order sandwich panel theory (HSAPT) approach, is the overall objective of this paper.

The main categorization adopted for the different approaches for the analysis of fully bonded sandwich panels includes sandwich structures with transversely incompressible core material (e.g. the textbooks and extended reviews by Plantema (1966), Allen (1969), Zenkert (1995), Vinson (1999), Noor et al. (1996) and Librescu and Hause (2000)), and transversely compressible core material following the HSAPT models (Frostig et al. (1992)) and similar ones. Fully bonded curved sandwich panels and shells with a transversely (radial) incompressible core have been considered by a few researchers, e.g. Librescu et al. (1994, 2000) for buckling and post buckling problems of sandwich shells subjected to thermal induced deformations, Vaswani et al. (1988) for vibration problems, Di Sciuva and Carrera (1990) and Rao and Meyer-Piening (1990) for buckling of sandwich shells. In addition, Hildebrand (1991), Smidt (1995), Tolf (1983) and Kant and Kommineni (1992) used FE models adopting the Reissner–Mindlin hypothesis, and Kuhhorn and Schoop (1992) adopted displacements distributions (third and second order polynomial) derived for flat sandwich panels, for the analysis of sandwich shells. The effects of the radial (transverse) flexibility of the core on the local and overall behaviour of the curved sandwich panels have been implemented through the use of the high-order sandwich panel theory (HSAPT) for curved panels assuming geometrical linearity, see Frostig (1999) and others. Geometrically non-linear effects were treated by Bozhevolnaya and Frostig (1997) and Bozhevolnaya (1998) for shallow sandwich panels, and Karyadi (1998) for cylindrical shells. In addition, Bozhevolnaya and Frostig (2001) treated the free vibration of curved panels, Thomsen and Vinson (2001) presented a design study on all composite sandwich aircraft fuselage structures, and Lyckegaard and Thomsen (2004, 2006) treated localized effects in the linear and non-linear response of straight and curved sandwich panels.

As indicated previously, the response of sandwich panel with an interfacial debond between face sheets and the core, at some specific region(s) along the panel circumference, denoted as a delamination or a disband or a debond, is of significant importance when assessing the safety of sandwich structures. The topic has been addressed for flat panels by analytical and experimental approaches such as: Somers et al. (1991) and Hwu and Hu (1992) investigated the effects of a predetermined delamination using the approach by Simitses et al. (1985), Zenkert (1991) has addressed the case of interface debonding in sandwich beams experimentally; Lin et al. (1996) proposed a simplified two-dimensional continuum model for a delaminated face sheet of a sandwich plate; Avery et al. (1998) presented an extensive experimental study of the buckling of delaminated sandwich panels, Kardomateas (1998) and Avile's and Carlsson (2005) considered buckling of a delaminated sandwich panel adopting an elastic foundation approach; Sridharan and Li (2006) used a cohesive layer approach to describe a debobded sandwich column and Avile's and Carlsson (2008) have determined failure characteristic of a debonded sandwich beam using a sandwich DCB specimen.

The topic of interface debonding in flat sandwich panels with a compliant core, and adopting the HSAPT approach, was addressed by Frostig (1992) and Frostig and Thomsen (2005) for the linear and non-linear response of flat delaminated panels, Frostig and Sokolinsky (2000) considered buckling of flat delaminated panels using a spring description to model a non-rigid bonding layer, delamination and slip layer, and Rabinovitch and Frostig (2002) considered the bending of delmaninated circular sandwich panels. The analysis of curved debonded sandwich panels based on HSAPT approach appear in Frostig et al. (2004) assuming a linear response.

The thermal and the thermo-mechanical non-linear response of a flat sandwich panel with a compliant core has been considered by Frostig and Thomsen (2008), along with the effect of the thermal degradation of the mechanical properties of the core, see Frostig and Thomsen (2007). A modified HSAPT approach has been used to analyse the non-linear thermo-mechanical response of curved sandwich panels, see Frostig and Thomsen (2009). This series of papers reveals that the radial (transverse) flexibility of the core plays a major role in the non-linear thermo-mechanical response of flat or curved sandwich panels. Thermal effects in curved sandwich panels have been considered by a few researchers assuming an incompressible core or other simplified computational models, see list of references in Frostig and Thomsen (2009).

In this paper, the mathematical formulation is based on the adoption of the high-order sandwich panel theory (HSAPT) approach to model the non-linear response of a curved sandwich panel with a finite length through-the-width debond (crack) located at one of the face sheet-core interfaces. The curved sandwich panel is subjected to mechanical, thermal and thermo-mechanical loading schemes. The complete sandwich structure is assumed to consist of fully bonded and debonded regions that are interconnected through compatibility and continuity conditions. The two curved face sheets are assumed to possess both membrane and flexural rigidities, and are modelled according to the Euler–Bernoulli hypothesis using non-linear kinematic relations that corresponds to large displacements with moderate rotations. The curved face sheets are interconnected through the enforcement of compatibility and equilibrium with a 2D compressible or extensible (i.e. compliant) elastic core. It is further assumed that the core material possesses shear and radial (through-thickness) normal stiffnesses only, while the circumferential (in-plane) stiffness is assumed to be negligible, see Frostig and Thomsen (2005) and Schwarts-Givli et al. (2007). Thus, the circumferential normal stresses within the core are neglected which allow the core to undergo large rigid body displacements with kinematic relations of small deformations. Shear and radial normal stresses exist within the core of a fully bonded interface region, while the core within the debonded region is free of shear stresses and radial normal stresses except for areas where contact exists between the faces and the core. In such areas the core can accommodate only compressive radial normal stresses. The loads are applied at the face sheets while the thermal loading is applied to all the constituents of the sandwich pane assembly.

The mathematical formulation presents the governing field equations of the debonded regions along with the appropriate boundary/continuity conditions as well as the thermal stress and the displacement fields within the core, where the core mechanical properties are assumed to be either temperature independent (*TI*) or temperature dependent (*TD*). A numerical study is followed and it demonstrates the mechanical, thermal and the thermo-mechanical non-linear response characteristics including also the influence of the length of the debonded region. The paper is concluded by a brief summary and the suggestion of some recommendations.

2. Mathematical formulation

The overall curved sandwich panel consists of fully bonded and debonded regions. Only the field equations and the boundary/

continuity conditions of the debonded regions are presented, since the field equations and boundary/continuity conditions for the fully bonded region can be derived as a special case hereof. The field equations and the boundary/continuity conditions of the debonded regions are derived following the steps of the HSAPT approach for the debonded flat and curved sandwich panels, see Frostig (1992), Frostig and Thomsen (2005), and Frostig et al. (2004), and using the variational principle of extremum of the total potential energy as follows:

$$\delta(U+V)=0 \tag{1}$$

where U is in the internal potential strain energy and V is the potential energy of the external loads.

The internal potential energy in terms of polar coordinates of the bonded and debonded regions reads:

$$\begin{aligned}\delta U=\sum_{k=1}^{n_{bon}}\Bigg(&\int_{\phi_{l_k}}^{\phi_{r_k}}\int_{-\frac{1}{2}}^{\frac{1}{2}d_j}\int_{-\frac{1}{2}b_w}^{\frac{1}{2}b_w}\sigma_{sst}(\phi,z_t)\delta\epsilon_{sst}(\phi,z_t)r_t\mathrm{d}y\,\mathrm{d}z_t\,\mathrm{d}\phi\\&+\int_{\phi_{l_k}}^{\phi_{r_k}}\int_{-\frac{1}{2}db}^{\frac{1}{2}db}\int_{-\frac{1}{2}b_w}^{\frac{1}{2}b_w}\sigma_{ssb}(\phi,z_b)\delta\epsilon_{ssb}(\phi,z_b)r_b\mathrm{d}y\,\mathrm{d}z_b\,\mathrm{d}\phi\\&+\int_{\phi_{l_k}}^{\phi_{r_k}}\int_{r_{bc}}^{r_{tc}}\int_{-\frac{1}{2}b_w}^{\frac{1}{2}b_w}(\tau_{rs}(\phi,r_c)\delta\gamma_{rs}(\phi,r_c)\\&+\sigma_{rr}(\phi,r_c)\delta\epsilon_{rr}(\phi,r_c))r_c\mathrm{d}y\,\mathrm{d}r_c\,\mathrm{d}\phi\Bigg)\\&+\sum_{n=1}^{n_{deb}}\Bigg(\int_{\phi_{l_n}}^{\phi_{r_n}}\int_{-\frac{1}{2}d_j}^{\frac{1}{2}d_j}\int_{-\frac{1}{2}b_w}^{\frac{1}{2}b_w}\sigma_{sst}(\phi,z_t)\delta\epsilon_{sst}(\phi,z_t)r_t\mathrm{d}y\,\mathrm{d}z_t\,\mathrm{d}_\phi\\&+\int_{\phi_{l_n}}^{\phi_{r_n}}\int_{-\frac{1}{2}db}^{\frac{1}{2}db}\int_{-\frac{1}{2}b_w}^{\frac{1}{2}b_w}\sigma_{ssb}(\phi,z_b)\delta\epsilon_{ssb}(\phi,z_b)r_b\mathrm{d}_y\,\mathrm{d}z_b\,\mathrm{d}\phi\\&+\int_{\phi_{l_n}}^{\phi_{r_n}}\int_{r_{bc}}^{r_{tc}}\int_{-\frac{1}{2}b_w}^{\frac{1}{2}b_w}\eta\sigma_{rr}(\phi,r_c)\delta\epsilon_{rr}(\phi,r_c)r_c\mathrm{d}y\,\mathrm{d}r_c\,\mathrm{d}\phi\Bigg)\end{aligned} \tag{2}$$

where $\sigma_{ssj}(\phi,r_j)$ and $\varepsilon_{ssj}(\phi,r_j)$ $(j=t,b)$ are the stresses and strains in the circumferential direction of the face sheets, respectively; $\tau_{rs}(\phi,r_c)=0$ (see Frostig et al. (2004)) are the core shear stresses, which are zero in the debonded region; $\sigma_{rr}(\phi,r_c)$ and $\varepsilon_{rr}(\phi,r_c)$ are the compressive radial normal stresses and strains, respectively, that exist only at contact areas; r and s refer to the circumferential and radial directions of the curved panel; α is the angle of the curved panel; $r_j(j=t,b,c)$ are the radii of the centroidal lines of the face sheets and the radial coordinate of the core, respectively; $r_{jc}(j=t,b)$ refers to the radii of the upper and the lower face-core interface lines, respectively, where $r_{tc}=r_t-d_t/2$ and $r_{bc}=r_b+d_b/2$; b_w and $d_j(j=t,b)$ are the width and the thicknesses of the face sheets, respectively; ϕ_{m_n} and $(m=l,r)$ are the left and the right angle coordinates of the bonded and debonded regions (see Fig. 1); η equals 1 in areas with contact and 0 in areas without contact; n_{bon} and n_{deb} are the number of bonded and debonded regions, respectively; and, finally, δ is the variational operator. For geometry, sign conventions, coordinates, deformations and internal resultants, see Fig. 1. Please notice that the shear stresses within the debonded regions are null since the debond crack faces are free of shear tractions; see Frostig (1992) and Frostig et al. (2004).

The variation of the potential energy of the external loads includes the external loads applied within the bonded and debonded regions as well as at the panel edges, and reads:

$$\begin{aligned}\delta V=&-\int_0^{\alpha}(n_t\delta u_{ot}(\phi)+q_t\delta w_t(\phi)+m_t(\phi)\delta\beta_t(\phi))r_t\mathrm{d}\phi\\&-\int_0^{\alpha}(n_b\delta u_{ob}(\phi)+q_b\delta w_b(\phi)+m_b(\phi)\delta\beta_b(\phi))r_b\mathrm{d}\phi\\&-\sum_{j=t}^{b}\Bigg(\sum_{i=1}^{Nc_j}\Bigg(\int_0^{\alpha}(N_{eij}(\phi)\delta u_{oj}(\phi)+P_{eij}(\phi)\delta w_j(\phi)\\&+M_{eij}(\phi)\delta\beta_j(\phi))\delta_D(\phi-\phi_i)\mathrm{d}\phi\Bigg)\Bigg)\end{aligned} \tag{3}$$

where n_j, q_j and m_j $(j=t,b)$ are the external distributed loads in the circumferential and radial directions, respectively, and the distributed bending moment applied at the face sheets; u_{oj} and $w_j(j=t,b)$ are the circumferential and radial displacements of the face sheets, respectively; β_j is the slope of the section of the face sheet; N_{eij}, P_{eij} and $M_{eij}(j=t,b)$ are the external concentrated loads in the circumferential and radial directions, respectively, and the concentrated bending moment applied at the face sheets at $s=s_{ij}$; $Nc_j(j=t,b)$ is the number of concentrated loads at the top and bottom faces,

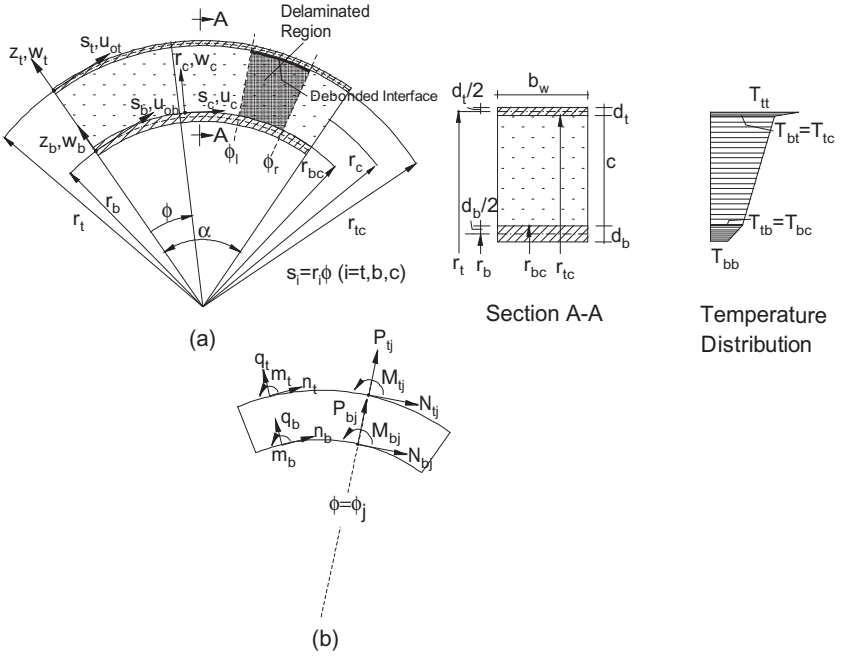

Fig. 1. Layout, dimensions, temperature distribution and signs conventions of a delaminated curved sandwich panel: (a) geometry; (b) loads at face sheets.

and $\delta_D(s_j - s_{ji})$ is the Dirac function at the location of the concentrated loads. It should be noted that the integration is conducted separately for the bonded and debonded regions, respectively. For sign conventions and definition of loads see Fig. 1.

The through-thickness distribution of the face sheet displacements follow the Euler–Bernoulli assumptions with negligible transverse shear strain and kinematic relations corresponding to large displacements and small rotations, and they read ($j = t,b$):

$$u_j(\phi, z_j) = u_{oj}(\phi) + z_j\beta_j(\phi), \quad \beta_j(\phi) = \frac{u_{oj}(\phi)}{r_j} - \frac{\frac{d}{d\phi}w_j(\phi)}{r_j} \tag{4}$$

where z_j is the radial coordinate measured *upward* from the centroid of each face sheet; r_j is the radius and $s_j = r_j\phi$ is the circumferential coordinate of the face sheets that have identical radial centre; and ϕ is the angle measured from the origin, see Fig. 1 for geometry. Hence, the strain distribution can be expressed in the form:

$$\epsilon_{ss_j}(\phi) = \epsilon_{ossj}(\phi) + z_j\chi_j(\phi) \tag{5}$$

where the face sheet mid-plane strains and curvatures equal:

$$\epsilon_{oss_j}(\phi) = \frac{d}{d\phi}u_{oj}(\phi) + \frac{w_j(\phi)}{r_j(\phi)} + \frac{1}{2}\beta_j(\phi)^2$$
$$\chi_j(\phi) = \frac{\frac{d}{d\phi}\beta_j(\phi)}{r_j} = \frac{\frac{d}{d\phi}u_{oj}(\phi)}{r_j^2} - \frac{\frac{d^2}{d\phi^2}w_j(\phi)}{r_j^2} \tag{6}$$

Adopting the approximation of small deformations, the kinematic relations for the core read:

$$\epsilon_{rr_c}(\phi, r_c) = \frac{\partial}{\partial r_c}w_c(\phi, r_c)$$
$$\gamma_c(\phi, r_c) = \frac{\partial}{\partial r_c}u_c(\phi, r_c) - \frac{u_c(\phi, r_c)}{r_c} + \frac{\frac{\partial}{\partial\phi}w_c(\phi, r_c)}{r_c} \tag{7}$$

where $w_c(\phi,r)$ and $u_c(\phi,r)$ are the radial and the circumferential core displacements, respectively.

The compatibility conditions corresponding to a fully bonded region requires ($j = t,b$) fulfilment of the following conditions:

$$u_c(r_{jc}, \phi) = u_{oj}(\phi) + \frac{1}{2}\frac{(-1)^k\left(u_{oj}(\phi) - \left(\frac{d}{d\phi}w_j(\phi)\right)\right)d_j}{r_j}$$
$$w_c(r_{jc}, \phi) = w_j(\phi) \tag{8}$$

where $k = 1$ when $j = t$, and $k = 0$ when $j = b$. Moreover, r_{jc} ($j = t,b$) are the radii of the upper and the lower face-core interfaces, respectively;and $u_c(r = r_{jc},\phi)$ and $w_c(r = r_{jc},\phi)$ are the core displacements in the circumferential and the radial directions at the face-core interfaces, respectively. In addition, when a debond is presentsat one of the face-core interfaces it is assumed that the other face-core interface is in full bond, which requires compatibility in the radial and circumferential directions.

The field equations and the appropriate boundary conditions are derived using the variational principle, see Eq. (1); the expressions for the variation of the internal and external potential energies, see Eqs. (2) and (3); the kinematic relations of the face sheets and the core, Eqs. (5)–(7); the compatibility requirements, see Eq. (8); and the stress resultants, see also Fig. 2. After integration by parts and some algebraic manipulations, the field equations for the bonded and debonded regions read:

Face sheets ($j = t,b$):

$$\eta\left(-\frac{1}{2}\frac{d_j}{r_j} + \gamma\right)\tau_{sr}(\phi, r = r_{jc})b_w r_{jc} + \frac{\left(u_{oj}(\phi) - \left(\frac{d}{d\phi}w_j(\phi)\right)\right)N_{ssj}(\phi)}{r_j} - \left(\frac{d}{d\phi}N_{ssj}(\phi)\right) + m_j(\phi) - \frac{\frac{d}{d\phi}M_{ssj}(\phi)}{r_j} - r_j n_j = 0$$

$$\left(1 + \frac{\frac{d}{d\phi}u_{oj}(\phi)}{r_j} - \frac{\frac{d^2}{d\phi^2}w_j(\phi)}{r_j}\right)N_{ssj}(\phi) + \left(-\frac{\frac{d}{d\phi}w_j(\phi)}{r_j} + \frac{u_{oj}(\phi)}{r_j}\right) \times \left(\frac{d}{d\phi}N_{ssj}(\phi)\right) - r_j q_t + r_{jc}\lambda\sigma_{rr}(\phi, r = r_{jc})b_w - \frac{1}{2}\frac{\eta r_{jc}b_w d_j\left(\frac{d}{d\phi}\tau_{sr}(\phi, r = r_{jc})\right)}{r_j} - \frac{\frac{d^2}{d\phi^2}M_{ssj}(\phi)}{r_j} + \frac{d}{d\phi}m_j(\phi) = 0 \tag{9}$$

Core:

$$\eta\left(\left(\frac{\partial}{\partial r_c}\tau_{sr}(\phi, r_c)\right)r_c + 2\tau_{sr}(\phi, r_c)\right) = 0$$

$$r_c\left(\frac{\partial}{\partial r_c}\sigma_{rr}(\phi, r_c)\right) + \sigma_{rr}(\phi, r_c) + \eta\frac{\partial}{\partial\phi}\tau_{sr}(\phi, r_c) = 0$$

where N_{ssj} and M_{ssj}($j = t,b$) are the in-plane stress and bending moment resultants of each face sheet, respectively; $\tau_{sr}(\phi, r = r_{jc})$ and $\sigma_{rr}(\phi, r = r_{jc})$ (with $j = t,b$) are the shear and radial normal stresses at the upper ad the lower face-core interface, respectively; $\lambda = 1$ for $j = t$ and $\lambda = -1$ for $j = b$; and $\eta = 0$ when the region has a delamination at one of its face-core interfaces (i.e. a *debonded* region), whereas $\eta = 1$ for a fully *bonded* region. Please notice that the independent variable in the face sheets is the circumferential angle ϕ and in the core it is the radial coordinate, r_c and ϕ. It should be noticed that due to the inclusion of geometrical non-linearity in the kinematic relations for the face sheets, the equilibrium (field) equations of the face sheets corresponds to deformed face sheet configurations, while the equilibrium (field) equations of the core, which is assumed to undergo only small deformations kinematic relations, corresponds to the undeformed core configuration, see Fig. 2. In addition, it should be noticed that within the debonded region only the second equation of the two equations for the core is used.

The boundary conditions for the various regions of the curved sandwich panel, where the loads and the constraints are defined in the circumferential and radial directions of each face sheet, respectively, as wells as at $\phi_e = 0,\alpha$, read:

Face sheets ($j = t,b$):

$$\left(\frac{M_{ssj}(\phi_e)}{r_j} + N_{ssj}(\phi_e)\right)\lambda - N_{ej} + \frac{M_{ej}}{r_j} = 0 \quad \textbf{or } u_{oj}(\phi_e) = u_{eoj}$$
$$-\frac{\lambda M_{ssj}(\phi_e)}{r_j} - \frac{M_{ej}}{r_j} = 0 \quad \textbf{or } w_{j,\phi}(\phi_e) = Dw_{ej}$$
$$\left(\left(\frac{D(w_j)(\phi_e)}{r_j} - \frac{u_{oj}(\phi_e)}{r_j}\right)N_{ssj}(\phi_e) + \frac{D(M_{ssj})(\phi_e)}{r_j} - m_j(\phi_e) + \frac{1}{2}\frac{\eta r_{jc}b_w d_j\tau_j(\phi_e)}{r_j}\right)\lambda - P_{ej} = 0 \quad \textbf{or } w_j(\phi_e) = w_{ej} \tag{10}$$

where $\lambda = 1$ for $\phi_e = \alpha$ and $\lambda = -1$ for $\phi_e = 0$; u_{eoj}, w_{ej} and Dw_{ej} are the prescribed circumferential and radial displacements, and the rotation at the edges of the upper and the lower face sheets, respectively; N_{ej}, P_{ej} and M_{ej} and are the imposed external loads; and $D(f)(\phi_e)$ denote a derivative at the prescribed coordinate ϕ_e. It should be noticed that the circumferential force condition, see the first of Eq. (10), is actually a combined stress resultant that results from moment equilibrium about the radial centre of each face sheet.

The boundary conditions of the core at $\phi_e = 0,\alpha$, and through the depth of the core at $r_{bc} \leqslant r_c \leqslant r_{tc}$, for a *bonded* and a *debonded* region read:

$$\tau_{rs}(\phi_e, r_c) = 0 \quad \textbf{or } \eta(w_c(\phi_e, r_c) - w_{ec}(r_c)) = 0 \tag{11}$$

where $w_{ec}(r)$ are prescribed deformations at the ends of the sandwich panel through the depth of the core. Here it is noticed that

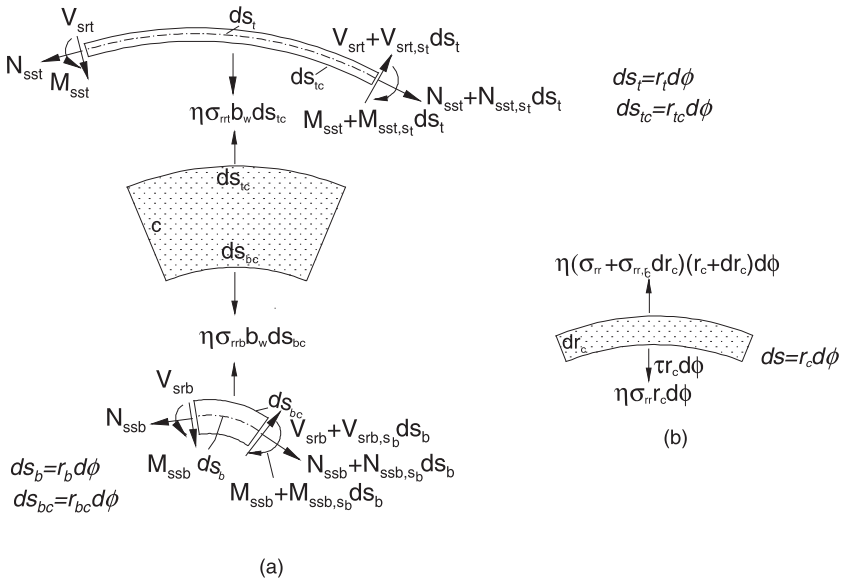

Fig. 2. Internal stress resultants and stresses within a debonded region of curved sandwich panel with contact: (a) stress resultants in face sheets on imposed on deformed face sheets; (b) stresses within the core.

only the left term in Eq. (11)) can be applied when the region is *debonded*, i.e. the condition of *zero* shear stress is imposed in this case. This means that there is no requirement for imposing continuity with respect to the radial displacement at the junction/transition between a fully *bonded* and a *debonded* region. It is possible to specify other types of edge conditions in the core than discussed above, like e.g. edge beams, but for detail please refer to Frostig and Thomsen (2009).

In order to determine the governing equations, see Eq. (9), the explicit description of the core stress and the displacement fields must be defined first, and this is considered in the forthcoming section.

2.1. Core displacement and stress fields

The explicit descriptions of the stress and displacement fields of the core are determined through the compatibility conditions, Eq. (8), applied on the following constitutive relations of radial normal and shear strains, see Eq. (7), for an isotropic core:

$$\epsilon_{rr}(\phi,r_c)=\frac{\sigma_{rr}(\phi,r_c)}{E_{rc}}+\alpha_{Tc}T_c(r_c,\phi),\quad \gamma_{sr}(\phi,r_c)=\frac{\tau_{sr}(\phi,r_c)}{G_{src}} \tag{12}$$

where E_{rc} and G_{src} are the Young's and shear modulii of the core in the radial direction; α_{Tc} and $T_c(\phi,r_c)$ are the coefficient of thermal expansion (CTE) of the core and the thermal field within the core, respectively.

The stress fields within the core are derived through the solution of the core field equations, see Eq. (9), that read:

$$\tau_{sr}(\phi,r_c)=\frac{\eta\tau_t(\phi)r_{tc}^2}{r_c^2},\quad \sigma_{rr}(\phi,r_c)=\frac{\eta\left(\frac{\mathrm{d}}{\mathrm{d}\phi}\tau_t(\phi)\right)r_{tc}^2}{r_c^2}+\frac{C_{w1}(\phi)}{r_c}$$
$$\tau_b(\phi)=\frac{\eta\tau_t(\phi)r_{tc}^2}{r_{bc}^2},\quad \sigma_{rrj}(\phi)=\frac{\eta\left(\frac{\mathrm{d}}{\mathrm{d}\phi}\tau_t(\phi)\right)r_{tc}^2}{r_{cj}^2}+\frac{C_{w1}(\phi)}{r_c}\quad (j=t,b) \tag{13}$$

where $C_{w1}(\phi)$ is a coefficient of integration to be determined through the compatibility conditions at the face-core interfaces, see Eq. (8); $\tau_j(\phi)$, and $\sigma_{rrj}(\phi)$ $(j=t,b)$ are the interfacial shear and radial normal stresses at the upper and the low face-core interfaces, respectively and $\tau_t(\phi)$ is the interfacial shear stress at the upper face-core interface and is also the generalized coordinate of the core for the *bonded* region.

The displacements fields of the core in the radial and circumferential directions are determined using the constitutive relations, Eq. (12), and the compatibility conditions, see Eq. (8). For the case of a *bonded* region only the upper face-core interface and the radial compatibility conditions at the lower interface must be considered, while for the *debonded* region only the two compatibility conditions in the radial direction and the compatibility condition in the circumferential direction at the bonded face-core interface should be used. The explicit description of the stress and displacements fields for the *bonded* regions appears in Frostig and Thomsen (2009). The stress and displacement fields for the *debonded* region, assuming that the core properties are *Temperature Independent (TI)*, read:

Radial normal stresses:

$$\sigma_{rr}(\phi,r_c)=-\frac{1}{2}\frac{(2w_b(\phi)-2w_t(\phi)+(T_{cb}+T_{ct})\alpha_c c)E_{cr}}{r_c\ln\left(\frac{r_{tc}}{r_{bc}}\right)}$$

$$\sigma_{rrt}(\phi,r_c)=-\frac{1}{2}\frac{(2w_b(\phi)-2w_t(\phi)+(T_{cb}+T_{ct})\alpha_c c)E_{cr}}{r_{tc}\ln\left(\frac{r_{tc}}{r_{bc}}\right)},$$
$$\sigma_{rrb}(\phi)=-\frac{1}{2}\frac{(2w_b(\phi)-2w_t(\phi)+(T_{cb}+T_{ct})\alpha_c c)E_{cr}}{r_{bc}\ln\left(\frac{r_{tc}}{r_{bc}}\right)} \tag{14}$$

Displacement fields:

$$\begin{aligned}w_c(\phi,r_c)=&\left(\left(\frac{1}{2}\frac{r_c^2}{c}-\frac{r_c r_{bc}}{c}\right)T_{ct}(\phi)+\left(-\frac{1}{2}\frac{r_c^2}{c}+r_c+\frac{r_c r_{bc}}{c}\right)T_{cb}(\phi)\right)\alpha_{Tc}\\&+\frac{C_{w1}(\phi)\ln(r_c)}{E_{rc}(\phi)}+C_{w2}(\phi)\\u_c(r_c,\phi)=&\left(\left(\frac{r_c r_{bc}\ln(r_c)}{c}-\frac{1}{2}\frac{r_c^2}{c}\right)\left(\frac{\mathrm{d}}{\mathrm{d}\phi}T_{ct}(\phi)\right)\right.\\&\left.+\left(-\frac{r_c r_{bc}\ln(r_c)}{c}+\frac{1}{2}\frac{r_c^2}{c}-r_c\ln(r_c)\right)\left(\frac{\mathrm{d}}{\mathrm{d}\phi}T_{cb}(\phi)\right)\right)\alpha_{Tc}\\&+\frac{\mathrm{d}}{\mathrm{d}\phi}C_{w2}(\phi)+r_c C_u(\phi)\\&-r_c\left(\frac{\mathrm{d}}{\mathrm{d}\phi}C_{w1}(\phi)\right)\left(-\frac{\ln(r_c)}{E_{rc}(\phi)r_c}-\frac{1}{E_{rc}(\phi)r_c}\right)\end{aligned} \tag{15}$$

where $\sigma_{rrj}(j=t,b)$ are the interfacial radial normal stresses at the upper and the lower face-core interfaces, respectively; $C_{w2}(\phi)$ and $C_u(\phi)$ are the coefficients of integration to be determined through

the compatibility conditions at the face–core interfaces, see Eq. (8). Please notice that within areas without contact the radial normal stresses are nill, thus implying that the radial and circumferential displacements within the core should be defined by the compatibility conditions corresponding to *full bonding* at the bonded interface.

For the case *without contact* the core stress and displacements fields for both *TI* and *TD* core properties read:

$$\sigma_{rr}(\phi,r_c)=0$$

$$\begin{aligned}w_c(\phi,r_c)&=C_{w1}(\phi)+\frac{1}{c}\left(\left(-\frac{1}{2}T_{ct}(\phi)+\frac{1}{2}T_{cb}(\phi)\right)\alpha_{Tc}r_c^2\right.\\&\left.+(T_{ct}(\phi)r_{tc}-T_{cb}(\phi)r_{bc})\alpha_{Tc}r_c\right)\\u_c(\phi,r_c)&=\left(\left(\frac{\ln(r_c)r_{bc}}{c}-\frac{1}{2}\frac{r_c}{c}\right)r_c\left(\frac{\mathrm{d}}{\mathrm{d}\phi}T_{cb}(\phi)\right)\right.\\&\left.+\left(\frac{1}{2}\frac{r_c}{c}-\frac{\ln(r_c)r_{tc}}{c}\right)r_c\left(\frac{\mathrm{d}}{\mathrm{d}\phi}T_{ct}(\phi)\right)\right)\alpha_{Tc}\\&+\left(C_u(\phi)+\frac{\frac{\mathrm{d}}{\mathrm{d}\phi}C_{w1}(\phi)}{r_c}\right)r_c\end{aligned}\tag{16}$$

where $C_{w1}(\phi)$ and $C_u(\phi)$ are coefficients of integration that are determined using the compatibility conditions at the bonded face-core interface, see Eq. (8).

The core displacement fields of a *debonded* region with full contact and *Temperature Dependent (TD)* mechanical properties, and using the radial stress fields from Eq. (13), read:

$$\begin{aligned}w_c(\phi,r_c)&=\left(\left(\frac{1}{2}\frac{r_c^2}{c}-\frac{r_cr_{bc}}{c}\right)T_{cb}(\phi)+\left(-\frac{1}{2}\frac{r_c^2}{c}+r_c+\frac{r_cr_{bc}}{c}\right)T_{ct}(\phi)\right)\alpha_{Tc}\\&+C_{w1}(\phi)\left(\int\frac{1}{r_cE_{rc}(\phi,r_c)}\mathrm{d}r_c\right)+C_{w2}(\phi)\end{aligned}$$

$$\begin{aligned}u_c(r_c,\phi)&=\left(\left(\frac{r_cr_{bc}\ln(r_c)}{c}-\frac{1}{2}\frac{r_c^2}{c}\right)\left(\frac{\mathrm{d}}{\mathrm{d}\phi}T_{ct}(\phi)\right)\right.\\&\left.+\left(-\frac{r_cr_{bc}\ln(r_c)}{c}+\frac{1}{2}\frac{r_c^2}{c}-r_c\ln(r_c)\right)\left(\frac{\mathrm{d}}{\mathrm{d}\phi}T_{cb}(\phi)\right)\right)\alpha_{Tc}\\&+\frac{\mathrm{d}}{\mathrm{d}\phi}C_{w2}(\phi)+r_cC_u(\phi)\\&-r_c\left(\frac{\mathrm{d}}{\mathrm{d}\phi}C_{w1}(\phi)\right)\left(-\frac{\ln(r_c)}{E_{rc}(\phi,r_c)r_c}-\frac{1}{r_cE_{rc}(\phi,r_c)}\right)\end{aligned}\tag{17}$$

where

$$E_{rc}(\phi,r_c)=E_{rc}(r_c)H(-\sigma_{rrt}(\phi))$$

and where $E_{rc}(r_c)$ is the radial modulus of elasticity of the core that depends on the temperature distribution through the depth of the core and H is an Heaviside (step) function. It should be noticed that the radial normal stresses at the upper and the lower face-core interfaces are defined by inserting the appropriate radii for r_c, see Fig. 1. In addition, a closed-form description of the displacements fields is possible when the inverse of the modulus of elasticity can be described by a polynomial as follows:

$$E_{rc}(r_c)=\frac{1}{\sum_{i=0}^{N_e}E_ir_c^i}\tag{18}$$

where N_e is the number of terms in the polynomial description. Hence, the core displacement fields when the temperature distribution within the core is linear read:

$$\begin{aligned}w_c(\phi,r_c)&=\left(\sum_{i=3}^{N_e}\frac{E_ir_c^i}{i}+\frac{1}{2}E_2r_c^2+E_0\ln(r_c)+E_1r_c\right)C_{w1}(\phi)\\&+\left(\left(\frac{1}{2}\frac{r_c^2}{c}-\frac{r_cr_{bc}}{c}\right)T_{ct}(\phi)+\left(-\frac{1}{2}\frac{r_c^2}{c}+r_c+\frac{r_cr_{bc}}{c}\right)T_{cb}(\phi)\right)\alpha_{Tc}\\&+C_{w2}(\phi)\end{aligned}$$

$$\begin{aligned}u_c(\phi,r_c)&=\left(\sum_{i=3}^{N_e}\left(-\frac{E_ir_c^{(i-1)}}{(i-1)i}\right)+\frac{E_0\ln(r_c)}{r_c}-E_1\ln(r_c)-\frac{1}{2}E_2r_c+\frac{E_0}{r_c}\right)\\&\times\left(\frac{\mathrm{d}}{\mathrm{d}\phi}C_{w1}(\phi)\right)r_c+\left(\left(\frac{r_cr_{bc}\ln(r_c)}{c}-\frac{1}{2}\frac{r_c^2}{c}\right)\left(\frac{\mathrm{d}}{\mathrm{d}\phi}T_{ct}(\phi)\right)\right.\\&\left.+\left(-\frac{r_cr_{bc}\ln(r_c)}{c}+\frac{1}{2}\frac{r_c^2}{c}-r_c\ln(r_c)\right)\left(\frac{\mathrm{d}}{\mathrm{d}\phi}T_{cb}(\phi)\right)\right)\alpha_{Tc}\\&+\frac{\mathrm{d}}{\mathrm{d}\phi}C_{w2}(\phi)+r_cC_u(\phi)\end{aligned}\tag{19}$$

Generally, in a fully *bonded* region the field equations consist of four equilibrium equations for the face sheets, see Eq. (9), and a fifth equation that is equal to the last compatibility condition at one of the face-core interfaces that corresponds to the five generalized coordinates, four displacements of the face sheets, u_{ot}, w_t, u_{ob}, w_b and the fifth the interfacial shear stress at the upper face-core interface, $\tau_t(\phi)$, for details see Frostig and Thomsen (2009). However, for the case of a *debonded* region with *contact* the system of field equations consist of only four equilibrium equations that corresponds to the four displacements of the face sheets, while the fifth equation is identically satisfied zero since only three compatibility conditions are required, i.e., the compatibility of the radial displacements at upper and lower face-core interfaces,respectively, and a compatibility condition in the circumferential direction at the bonded interface.

2.2. Governing equations

For simplicity, it is assumed that the face sheets are homogeneous, isotropic and linear elastic, the temperature distribution through the depth of the face sheets and the core is linear and through the use of the following constitutive (load–displacement relations ($j=t,b$):

$$\begin{aligned}N_{ssj}(\phi)&=EA_j\left(\frac{\frac{\mathrm{d}}{\mathrm{d}\phi}u_{oj}(\phi)+w_j(\phi)}{r_j}+\frac{1}{2}\frac{\left(u_{oj}(\phi)-\left(\frac{\mathrm{d}}{\mathrm{d}\phi}w_j(\phi)\right)\right)^2}{r_j^2}\right.\\&\left.-\alpha_{Tj}\left(\frac{1}{2}T_{jt}(\phi)+\frac{1}{2}T_{jb}(\phi)\right)\right)\\M_{ssj}(\phi)&=EI_j\left(\frac{\frac{\mathrm{d}}{\mathrm{d}\phi}u_{oj}(\phi)-\left(\frac{\mathrm{d}^2}{\mathrm{d}\phi^2}w_j(\phi)\right)}{r_j^2}-\frac{\alpha_{Tj}(T_{jt}(\phi)-T_{jb}(\phi))}{d_j}\right)\end{aligned}\tag{20}$$

The complete set of governing equations for a *debonded* region with *contact* and uniform temperature distribution in face sheets can be expressed as a set of coupled first order ordinary differential equations as follows:

$$\begin{aligned}\frac{\mathrm{d}}{\mathrm{d}\phi}N_{sst}(\phi)&=-V_{srt}(\phi)-r_tn_t\\\frac{\mathrm{d}}{\mathrm{d}\phi}u_{ot}(\phi)&=\left(\frac{N_{sst}(\phi)}{EA_t(\phi)}-\frac{1}{2}\frac{(u_{ot}(\phi)-dw_t(\phi))^2}{r_t^2}\right)r_t-w_t(\phi)\\\frac{\mathrm{d}}{\mathrm{d}\phi}V_{srt}(\phi)&=-\frac{1}{2}\frac{1}{\ln\left(\frac{r_{bc}}{r_{tc}}\right)}(E_{cr}(\phi)H(-\sigma_{rrt}(\phi))(2w_b(\phi)-2w_t(\phi)\\&+cT_{cb}(\phi)\alpha_{T_c}+cT_{ct}(\phi)\alpha_{T_c})b_w)+N_{sst}(\phi)-r_tq_{rt}\\\frac{\mathrm{d}}{\mathrm{d}\phi}M_{sst}(\phi)&=r_tV_{srt}(\phi)+N_{sst}(\phi)u_{ot}(\phi)-N_{sst}(\phi)dw_t(\phi)+r_tmb_{t'}\\\frac{\mathrm{d}}{\mathrm{d}\phi}w_t(\phi)&=dw_t(\phi)\\\frac{\mathrm{d}}{\mathrm{d}\phi}dw_t(\phi)&=-\frac{M_{sst}(\phi)r_t^2}{EI_t(\phi)}+\left(\frac{N_{sst}(\phi)}{EA_t(\phi)}-\frac{1}{2}\frac{(u_{ot}(\phi)-dw_t(\phi))^2}{r_t^2}\right)r_t-w_t(\phi)\end{aligned}\tag{21}$$

$$\frac{\mathrm{d}}{\mathrm{d}\phi}N_{ssb}(\phi) = -V_{srb}(\phi) - r_b n_b,$$

$$\frac{\mathrm{d}}{\mathrm{d}\phi}u_{ob}(\phi) = \left(\frac{N_{ssb}(\phi)}{EA_b(\phi)} - \frac{1}{2}\frac{(u_{ob}(\phi) - dw_b(\phi))^2}{r_b^2}\right)r_b - w_b(\phi)$$

$$\frac{\mathrm{d}}{\mathrm{d}\phi}V_{srb}(\phi) = -\frac{1}{2}\frac{1}{\ln\left(\frac{r_{bc}}{r_{tc}}\right)}(E_{cr}(\phi)H(-\sigma_{rrt}(\phi))(2w_b(\phi) - 2w_t(\phi) + cT_{cb}(\phi)\alpha_{T_c} + cT_{ct}(\phi)\alpha_{T_c})b_w) + N_{ssb}(\phi) - r_b q_{zb}$$

$$\frac{\mathrm{d}}{\mathrm{d}\phi}M_{ssb}(\phi) = r_b V_{srb}(\phi) + N_{ssb}(\phi)u_{ob}(\phi) - N_{ssb}(\phi)dw_b(\phi) + r_b m b_b$$

$$\frac{\mathrm{d}}{\mathrm{d}\phi}w_b(\phi) = dw_b(\phi)$$

$$\frac{\mathrm{d}}{\mathrm{d}\phi}dw_b(\phi) = -\frac{M_{ssb}(\phi)r_b^2}{EI_b(\phi)} + \left(\frac{N_{ssb}(\phi)}{EA_b(\phi)} - \frac{1}{2}\frac{(u_{ob}(\phi) - dw_b(\phi))^2}{r_b^2}\right)r_b - w_b(\phi)$$

where H is a Heaviside (step) function and the generalized coordinate used here, with first-order ODES, are: u_{oj}, w_j, dw_j, N_{ssj}, M_{ssj} and $V_{srj}(j = t,b)$ where the first three corresponds to the circumferential, radial displacements and the slope of the radial displacement, and the last three correspond to the stress resultant in the circumferential direction, the bending moment resultants and the radial shear resultants of the upper and the lower face sheets respectively. Here it should be noticed that the number of governing equations is only 12, whereas the number of equations is 14 for the case of a *fully boned* region, see Frostig and Thomsen (2009). Thus the continuity conditions at the bonded/debonded edge of a *bonded* region requires a null shear stress of the core $\tau_t(\phi)$ region and full continuity with all other generalized coordinate mentioned above. Notice also that the governing equations for the case of a *debonded* region *without contact* are the same as those for the case of *contact* but with $\sigma_{rrt}(\phi) = 0$ and $H(-0.) = 0$.

Comments (*debonded region*):

1. For the case of *contact* the four governing equations are coupled, while for the case *without contact* the two governing equations for each face sheet are not coupled with those of the other face sheet, and the only interaction between the face sheets is a result of the continuity conditions imposed at the tips of the *debonded* region.
2. The continuity conditions within a *debonded* region for areas with *contact* and *without contact* are the same and in terms of the generalized coordinate of the face sheets only.
3. Closed-form solutions for the core stress and displacements fields exist when the inverse of the modulus of elasticity of the core is described by a polynomial.
4. The radial normal stresses are *non-uniform* through the thickness of the core when *contact* exists.

The response of a *debonded* sandwich panel is actually a combination of the response of the *bonded* regions interconnected, through equilibrium and continuity conditions, with *debonded* regions that consist of areas with and without *contact*. The exact location of the areas of *contact* are determined through the nonlinear solution of the governing equations of the *debonded* region, see Eq. (21). The area with *contact* is defined by its compressive radial normal stresses, see Eq. (14). Otherwise the area is considered as *without contact*.

The numerical solution of the non-linear governing set of differential equations can be achieved using numerical schemes such as the multiple-point shooting method, see Stoer and Bulirsch (1980), or the finite-difference (FD) approach using trapezoid or mid-point methods with Richardson extrapolation or deferred corrections, see Ascher and Petzold (1998), as implemented in Maple, see Char et al. (1991), along with parametric or arc-length continuation methods, see Keller (1992). Here, the FD approach implemented in Maple has been used successfully without any numerical instabilities even when the core rigidity has degraded significantly.

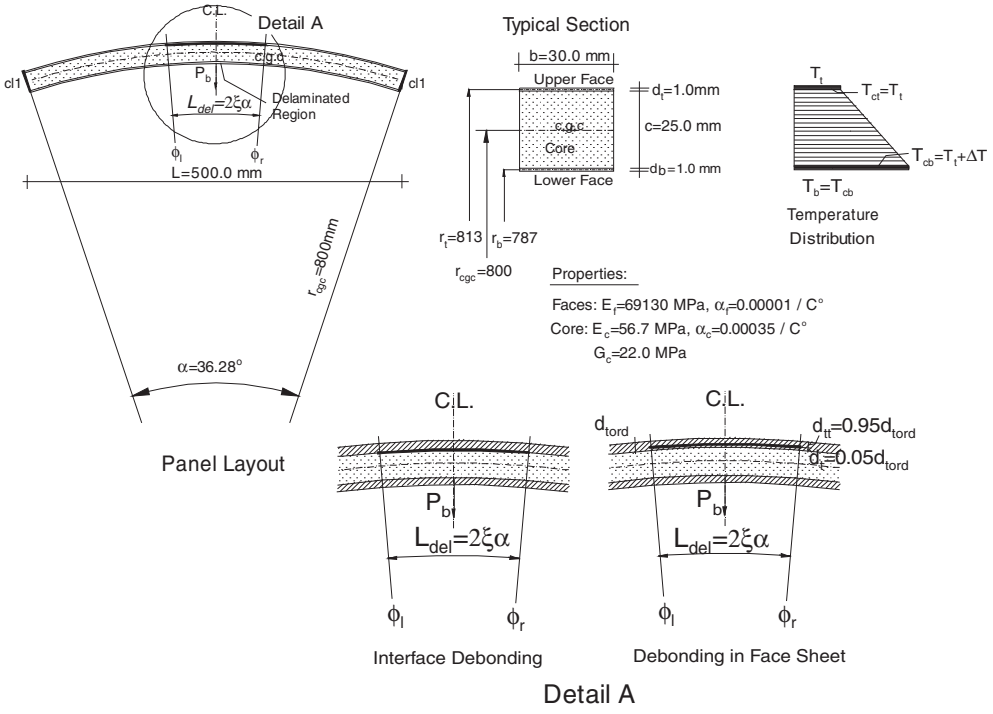

Fig. 3. Geometry, dimensions, mechanical properties, temperature distribution and debonding regions of the investigated debonded curved sandwich panel.

3. Numerical study

The numerical study presents and discusses the thermo-mechanical non-linear response of a delaminated sandwich panel when subjected to concentrated (point loading), see Fig. 3. The sandwich panel consists of two aluminium face sheets with a thickness of 1 mm, a coefficient of thermal expansion (CTE) $\alpha_{T_{t,b}} = 0.00001\ 1/C^o$. The core material is a DivinycellHD60 grade PVC foam with $E_c = 56.7$ MPa, $G_c = 22$ MPa, thickness 25 mm, and $\alpha_{T_c} = 0.00035\ 1/C^o$, see DIAB Divinycell (2003). The geometry of the curved sandwich panel corresponds to the experimental set-up described by Bozhevolnaya and Frostig (1997), and Bozhevolnaya (1998), see Fig. 3 for details. The delamination is assumed to be located at the upper face-core interface and is symmetric with respect to mid-span. The supporting system prevents circumferential displacements, in addition to the enforcement of constraints corresponding to simple supports (*ss1*) or a clamping condition (*cl1*).

The mechanical response of a debonded curved sandwich panel subjected to a concentrated load at mid-span of the lower face sheet, and without inclusion of thermal effects is studied first. This is followed by an investigation of the thermal response without mechanical loading, after which the introduction of the combined thermo-mechanical load response is given. Finally, the effects of including thermal degradation of the core properties on the thermo-mechanical responses are studied. The analyses assume geometric symmetry whenever possible.

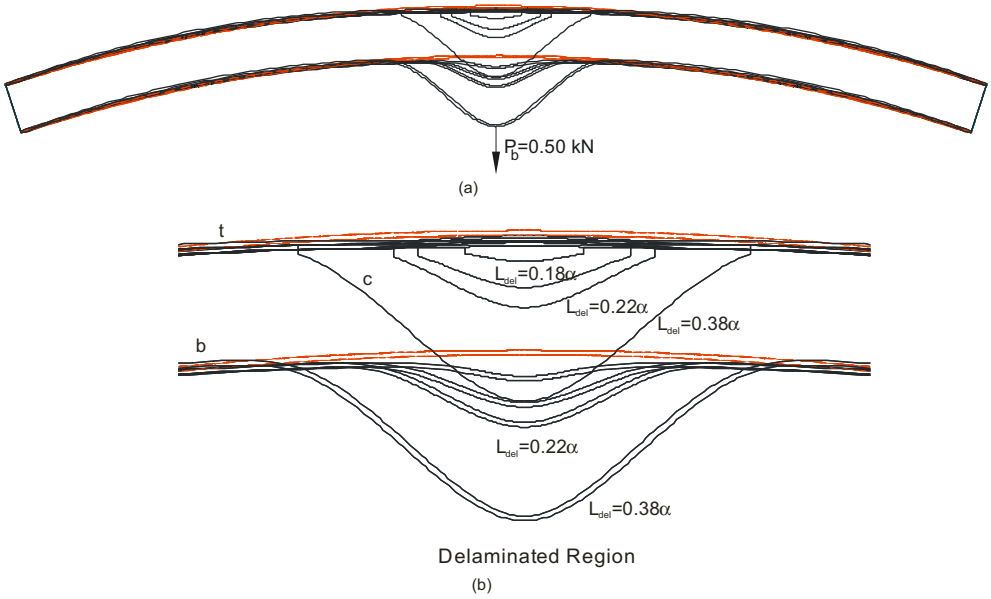

Fig. 4. Deformed shapes corresponding to a *linear* response of a debonded curved sandwich panel that is delaminated at its upper face-core interface, for different debond lengths: (a) overall shapes; (b) shapes in vicinity of debonded region.

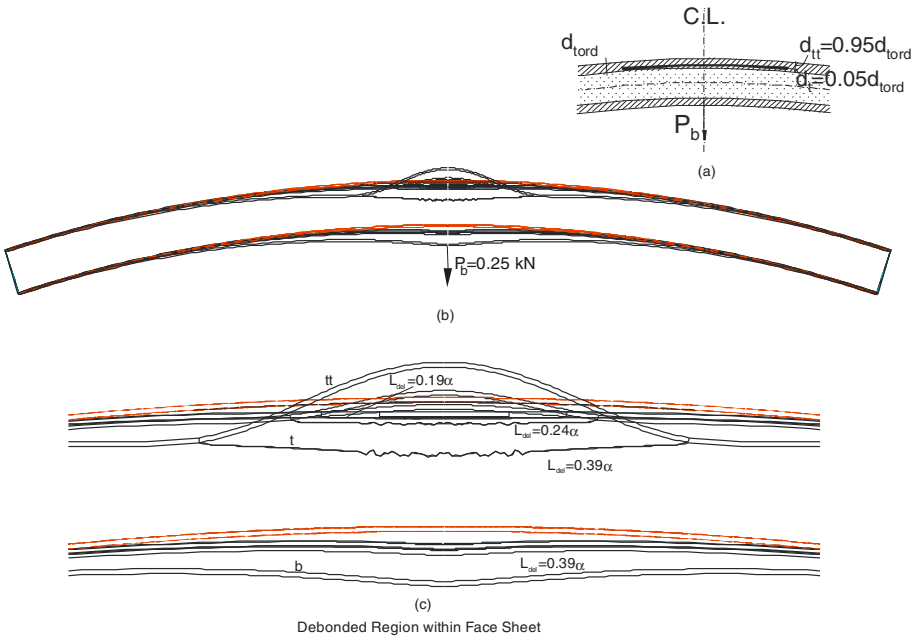

Fig. 5. Deformed shapes corresponding to a *non-linear* response of a debonded curved sandwich panel with a delamination located within the upper face sheet near its lower outer fibre, for different debonding lengths: (a) geometry – delamination; (b) overall shapes; (b) shapes in vicinity of delamination.

3.1. Temperature independent mechanical properties

3.1.1. Mechanical loading only

The mechanical response of a curved sandwich panel subjected to a concentrated load applied at mid-span of the lower face sheet appears in Figs. 4–7. The results include the deformed shape and the variation of various structural quantities plotted along the panel half span for various lengths of the debonded region. In addition, the strain energy release rate (ERR), which is defined as $G = \frac{\partial}{\partial a} U(\phi, r_c, a)$, where a is the length of the debonded region and U is internal energy, and the interfacial shear and radial normal stresses at the debonded region tips are presented. The ERR values are determined numerically using the finite differences approach. The analysis used here assumes small deformations with no contact. For the considered case, the actual response involves no contact between the crack surfaces in the debonded region, due to loading setup and the location of the debond crack at the upper face-core interface.

The deformed shapes of a simply-supported debonded panel appear in Fig. 4 for various lengths of the debonding regions. The overall deformed shape appears in Fig. 4a, with zoomed in results shown in Fig. 4b. The results reveal no contact within the debonded region and that the deformations increase as the length of the debonded region increases. In addition, it should be notices that there is a discontinuity in the radial displacement at the tips of the debonded crack which is a result of the computational model used, see Eq. (11). In reality, continuity of the displacements should be imposed at the crack tips, but it may involve very steep displacement gradients closed by. To validate that very large gradients are actually present, a similar computational model is used to determine the response of a delaminated curved sandwich panel where the debond crack is located near the lower fibre of the upper face sheet but within the face sheet, see Fig. 5a. The computational model for this case, which is omitted herein for brevity, imposes continuity conditions for the displacements in the radial and circumferential directions, respectively. The results of this model reveal a deformed shape that is very similar to that obtained for a sandwich panel with a debond crack at the upper face-core interface as shown in Fig. 4, but here the displacements are continuous and with very large gradients at the crack tips, see Fig. 5b and c.

Fig. 6a–d describes the variation of the radial displacements, the face sheet bending moment resultants, the face-core interface shear stresses, and finally the face-core interface radial normal stresses along half the sandwich panel circumference. The radial displacement pattern appears in Fig. 6a, and it is seen that the radial displacements become very large as the length of the debonded region is increased. The bending moment resultants in the face sheets, see Fig. 6b, display very large values at the edges of the delaminated region at the lower face sheet. It is due to the concentrated load, which is applied at mid-span of the lower face sheet,

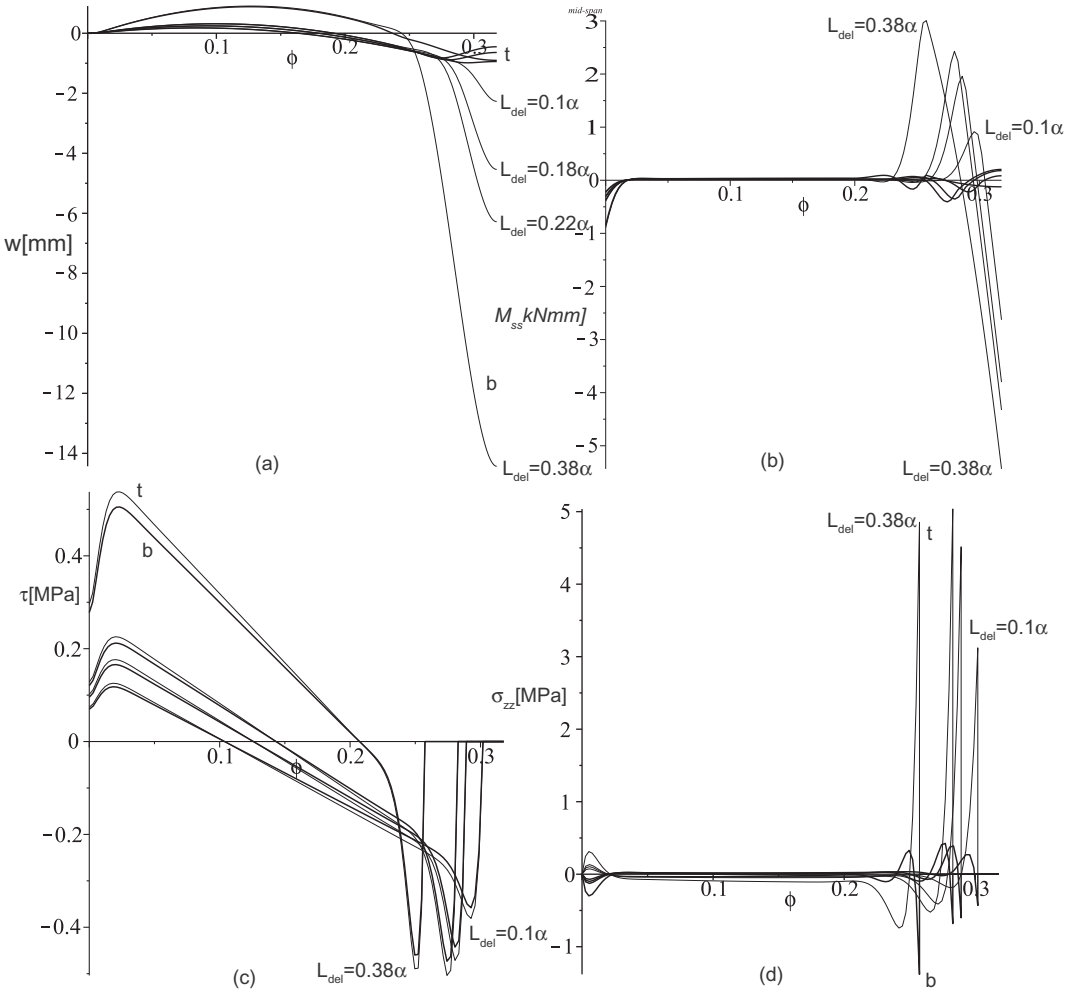

Fig. 6. The results of a *linear* mechanical response along half of the panel for different debond lengths: At the face sheets: (a) radial displacements; (b) bending moment resultants; and at the upper and lower face-core interfaces: (c) shear stresses; (d) radial normal stresses. Legend: ____ (thick) upper face/interface, ____ (thin) lower face/interface.

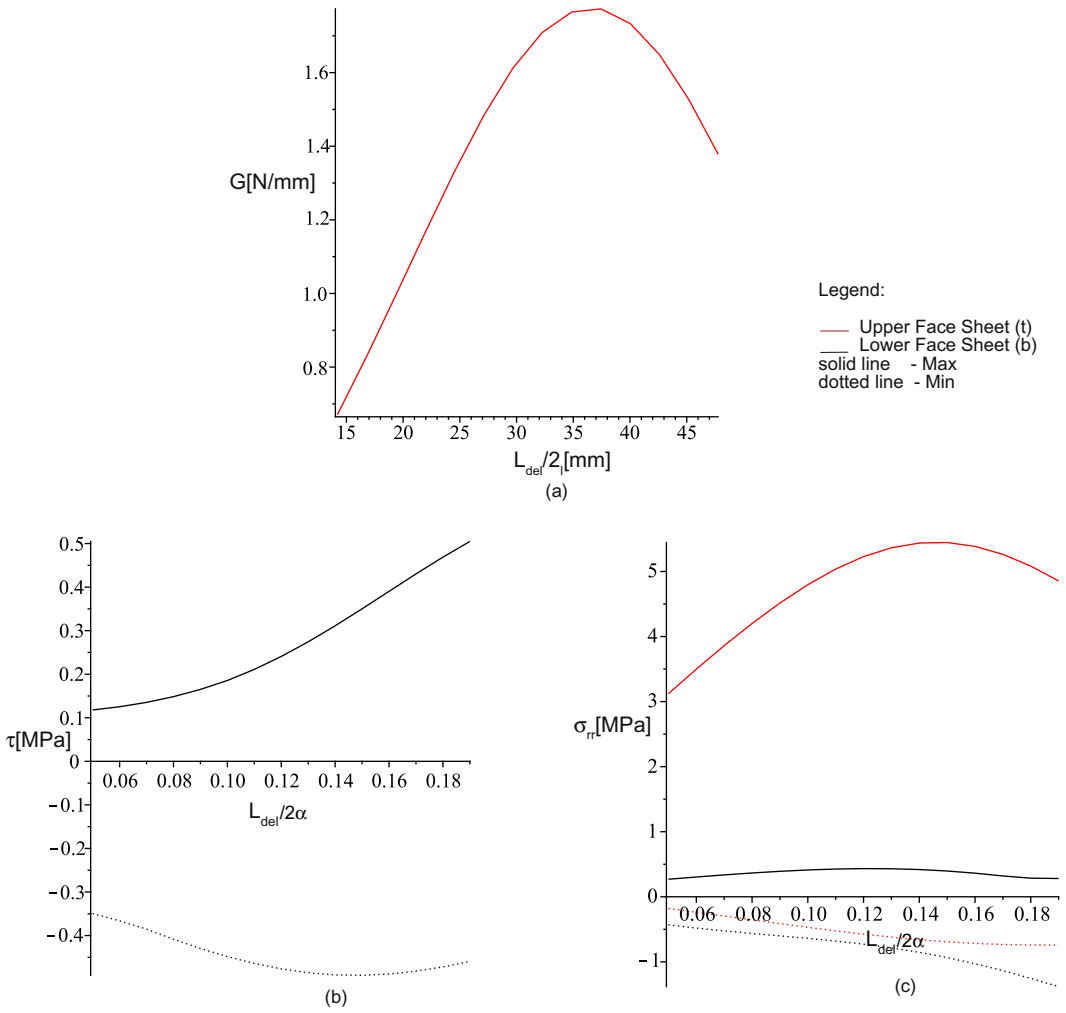

Fig. 7. Strain energy release rate (ERR) and extremum interfacial stresses corresponding to a *linear* response of a debonded panel: (a) ERR; (b) interfacial shear stresses; (c) interfacial radial normal stresses. Legend: black – upper face sheet, red — lower face sheet, solid – maximum . . .. – minimum. (For interpretation of the references to colour in this figure legend, the reader is referred to the web version of this article.)

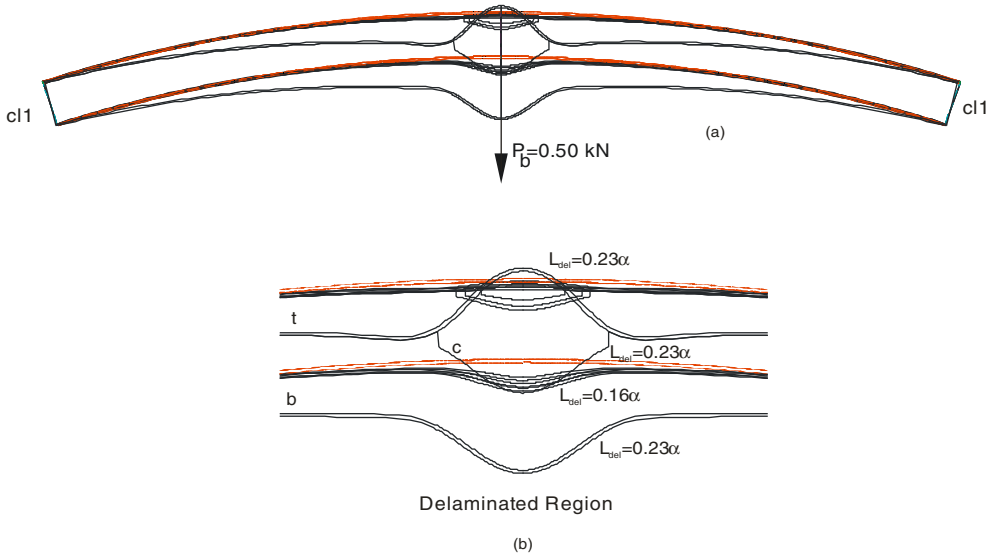

Fig. 8. Deformed shapes corresponding to a *non-linear* response of a debonded curved panel with a delamination at its upper face-core interface, for different debond lengths: (a) overall shapes; (b) shapes in vicinity of debonded region.

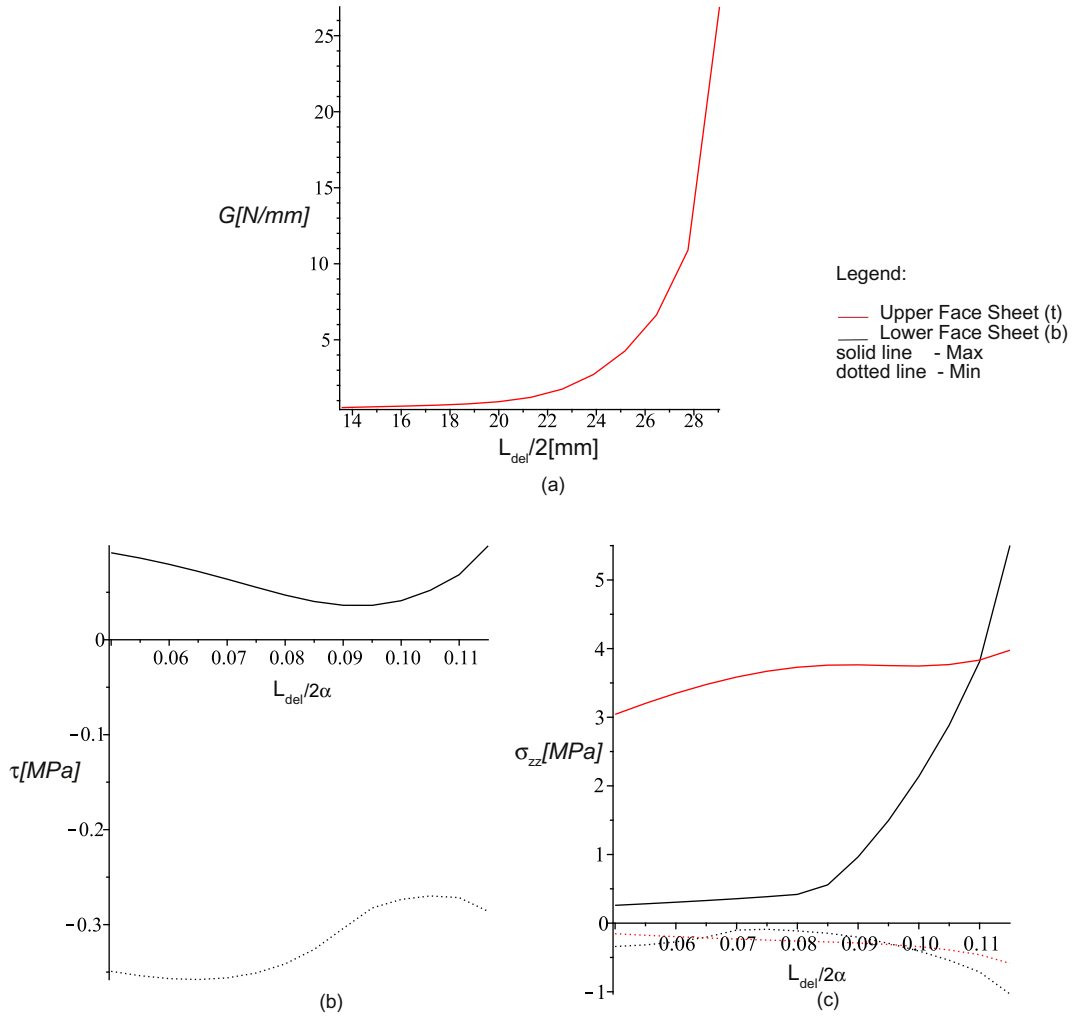

Fig. 9. Strain energy release rate (ERR) and extremum interfacial stresses corresponding to a *non-linear* response of a debonded panel: (a) ERR; (b) interfacial shear stresses; (c) interfacial radial normal stresses. Legend: black – upper face sheet, red — lower face sheet, solid – maximum . . . – minimum. (For interpretation of the references to colour in this figure legend, the reader is referred to the web version of this article.)

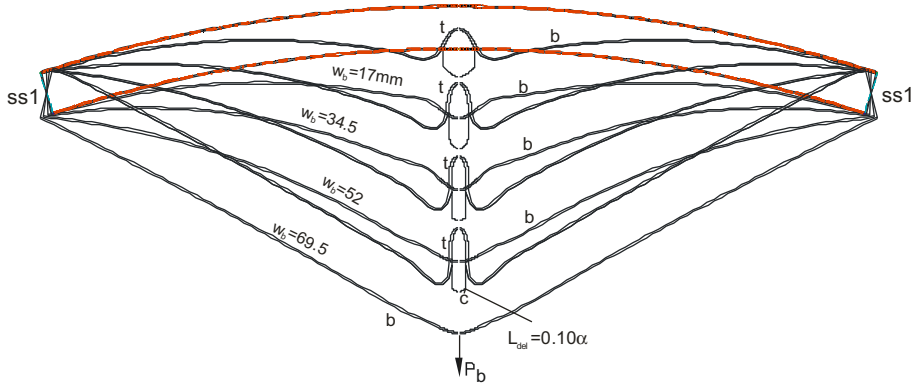

Fig. 10. Deformed shapes of a simply-supported and debonded ($L_{deb} = 0.10\alpha$) curved sandwich panel for different concentrated load levels.

and is transferred into the fully bonded regions through bending of the lower face sheet within the debonded region. The interfacial shear stresses at the upper and the lower interfaces appear in Fig. 6c, and it is observed that very large shear stress values are predicted at the crack tip, whereas the interface shear stresses are zero within the debonded region. Fig. 6d displays the normal interfacial radial stresses with extreme values appearing at the crack tips, whereas they are zero within the debonded region.

The calculated ERR (G) values and the extreme values of the interfacial shear and radial normal stresses appear in Fig. 7 for various lengths of the debonded region. The ERR curve, see Fig. 7a, reveals that at a certain length a maximum value is observed. Similar

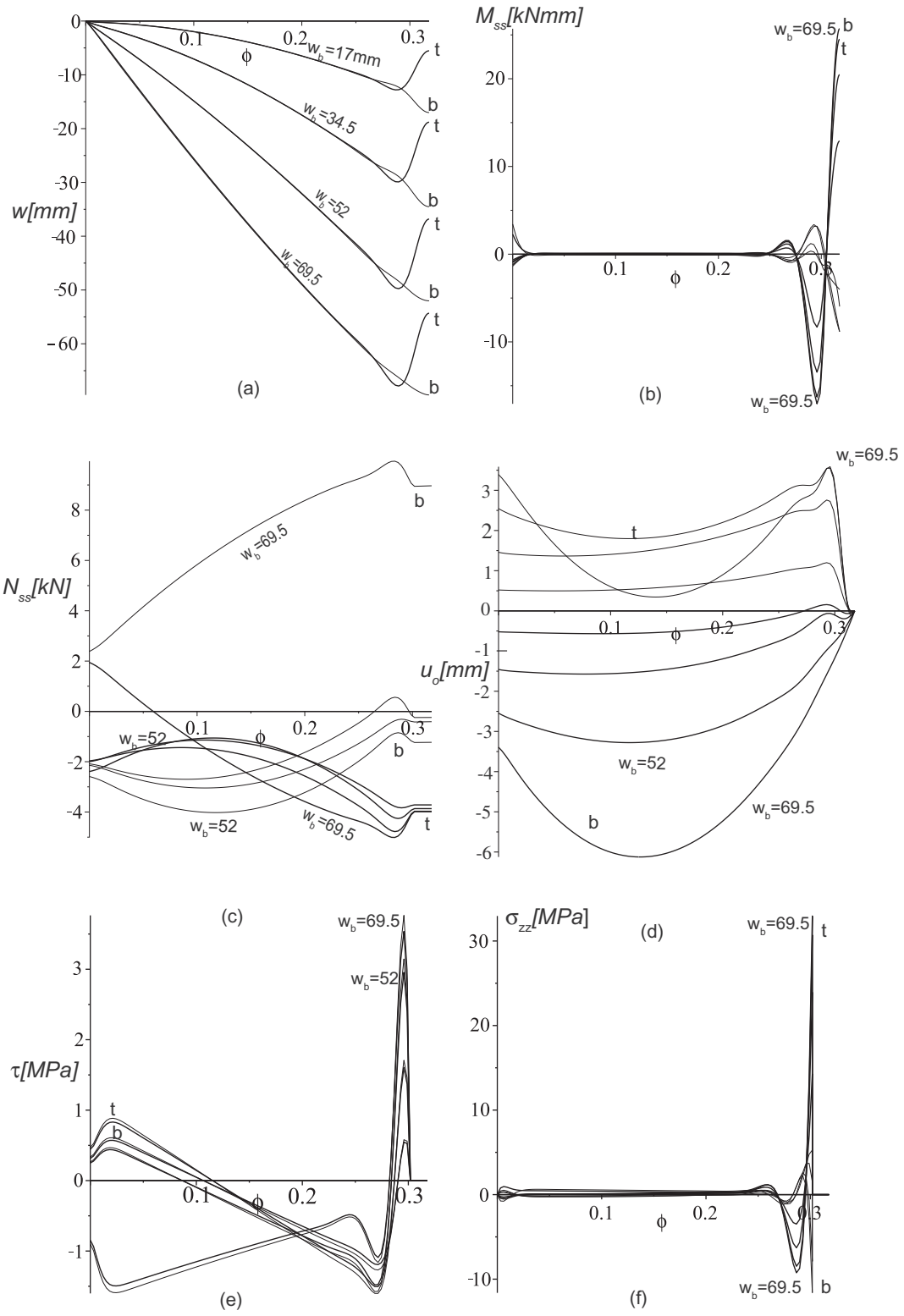

Fig. 11. Results corresponding to a *non-linear* mechanical response of a debonded ($L_{deb} = 0.10\alpha$) sandwich panel along half of the span for different loads: At the face sheets: (a) radial displacements; (b) bending moments; (c) circumferential stress resultants; (d) circumferential displacements; and at upper and lower face-core interfaces: (d) shear stresses; (e) radial normal stresses. Legend: ____ (thick) upper face/interface, ____ (thin) lower face/interface.

trends are observed for the interfacial radial normal stresses at the crack tips, see Fig. 7c. The interfacial shear stresses at crack tips, see Fig. 7b, increase as the length of the debond crack increases.

A similar case is presented in Figs. 8 and 9, but here a geometrical non-linear analysis is considered where the deformations are large and the rotations are of moderate magnitude. The results are presented for various lengths of the debond crack, but for somewhat smaller crack lengths compared with the linear case since the non-linear analysis procedure encounters numerical difficulties for large debond lengths. The deformed shape, see Fig. 8, reveal

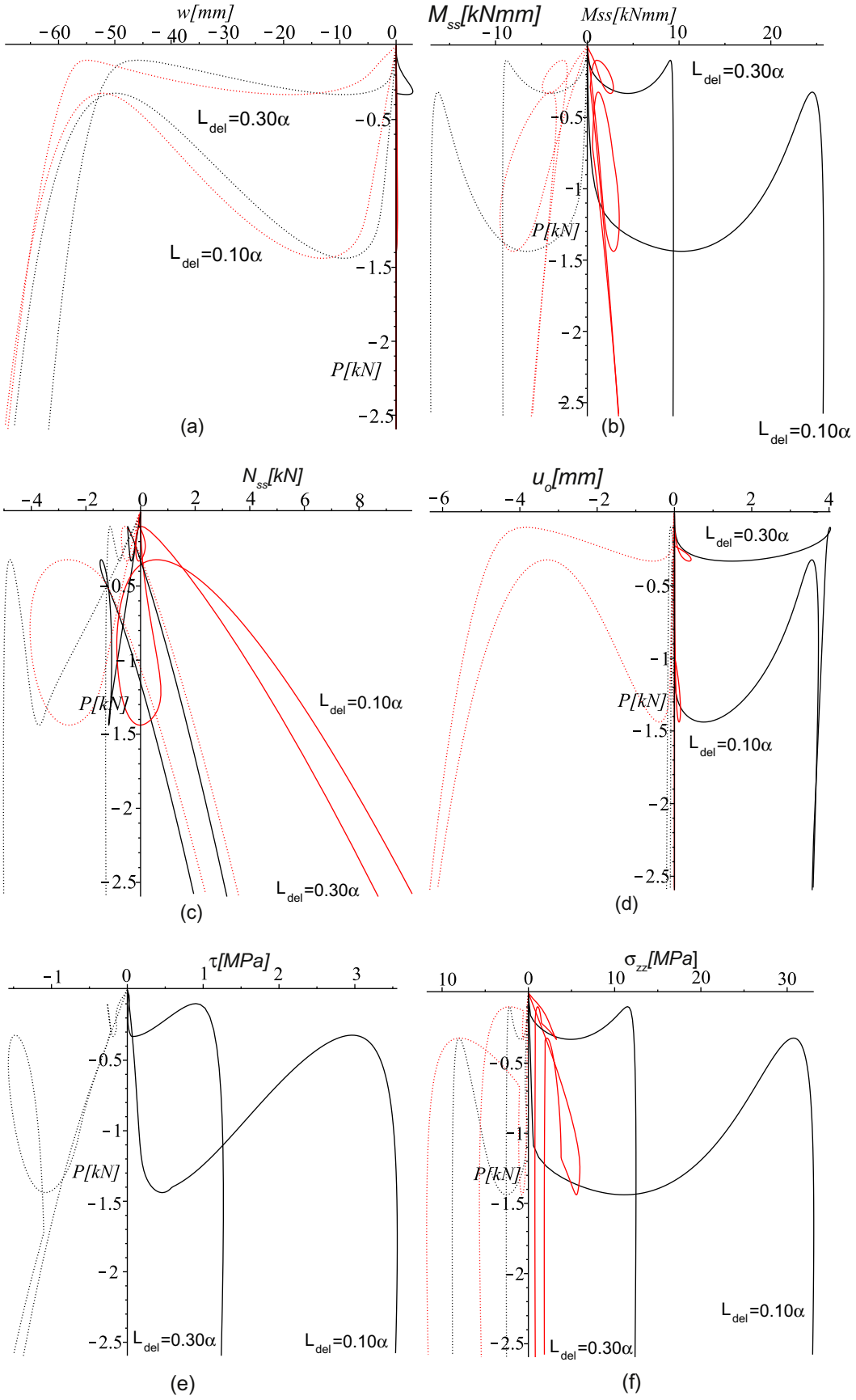

Fig. 12. Equilibrium curves for a debonded ($L_{deb} = 0.10\alpha$, 0.30α) curved sandwich panel showing concentrated load versus extreme structural values: At the face sheets: (a) radial displacements; (b) bending moment resultants; (c) circumferential stress resultants; (d) circumferential displacements; and at upper and lower face-core interfaces: (d) shear stresses; (e) radial normal stresses. Legend: black – upper face sheet, red — lower face sheet. (For interpretation of the references to colour in this figure legend, the reader is referred to the web version of this article.)

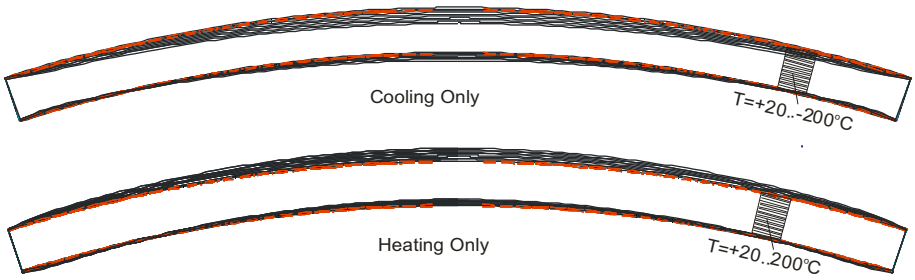

Fig. 13. Deformed shapes of thermally loaded (heating and cooling) debonded curved sandwich panel.

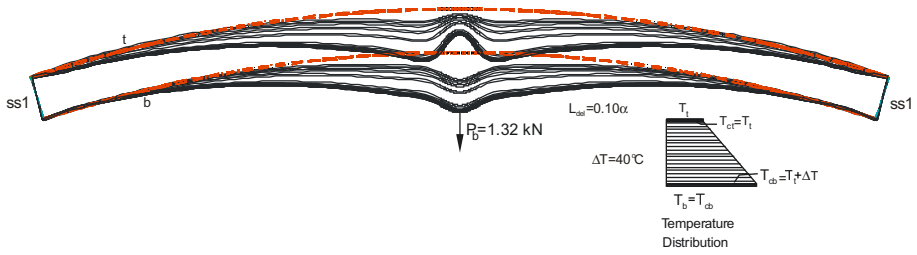

Fig. 14. Deformed shapes of a debonded curved sandwich panel subjected to thermo-mechanical loading in the form of a concentrated load and a radial thermal gradient loading for different temperatures at the upper face sheet.

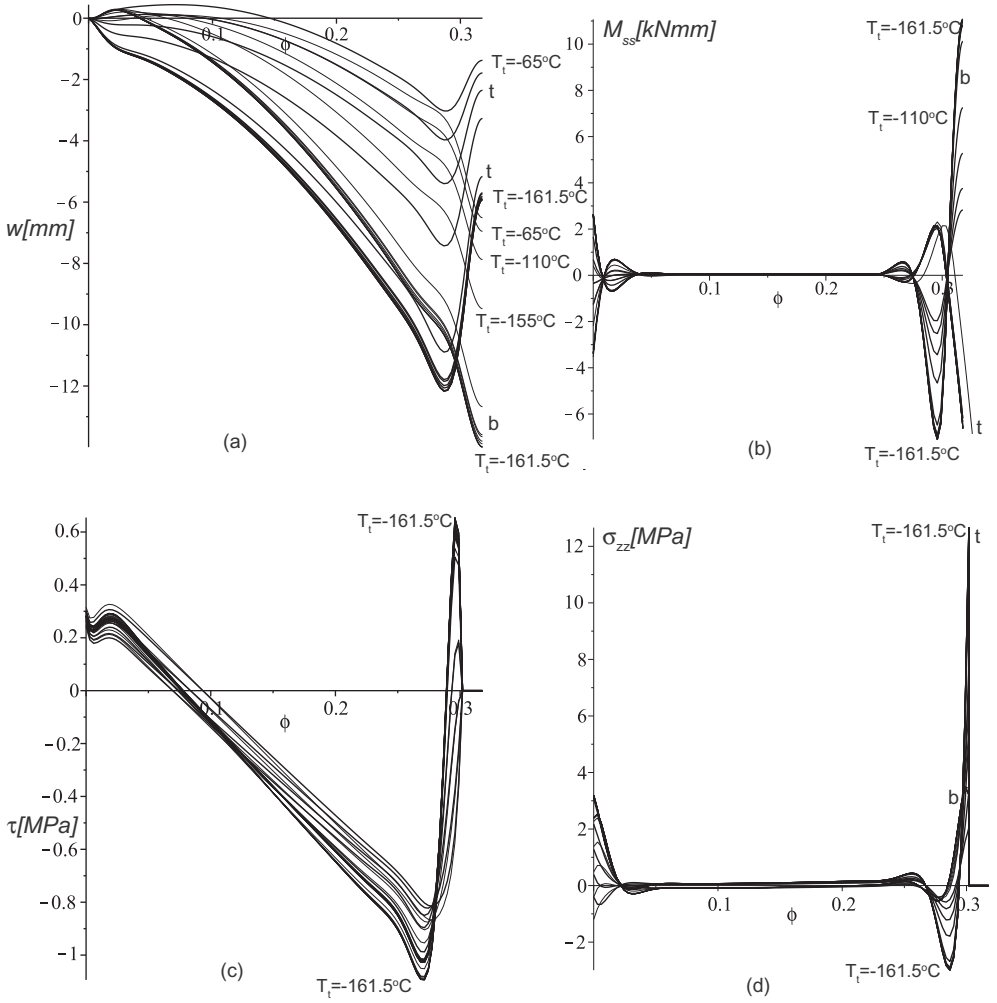

Fig. 15. Thermo-mechanical response results along the half of a debonded (L_{deb} = 0.10α) for different uniform temperatures: At the face sheets: (a) radial displacements; (b) bending moment resultants; and at upper and lower face-core interfaces: (c) shear stresses; (d) radial normal stresses. Legend: ____ (thick) upper face/interface, ____ (thin) lower face/interface.

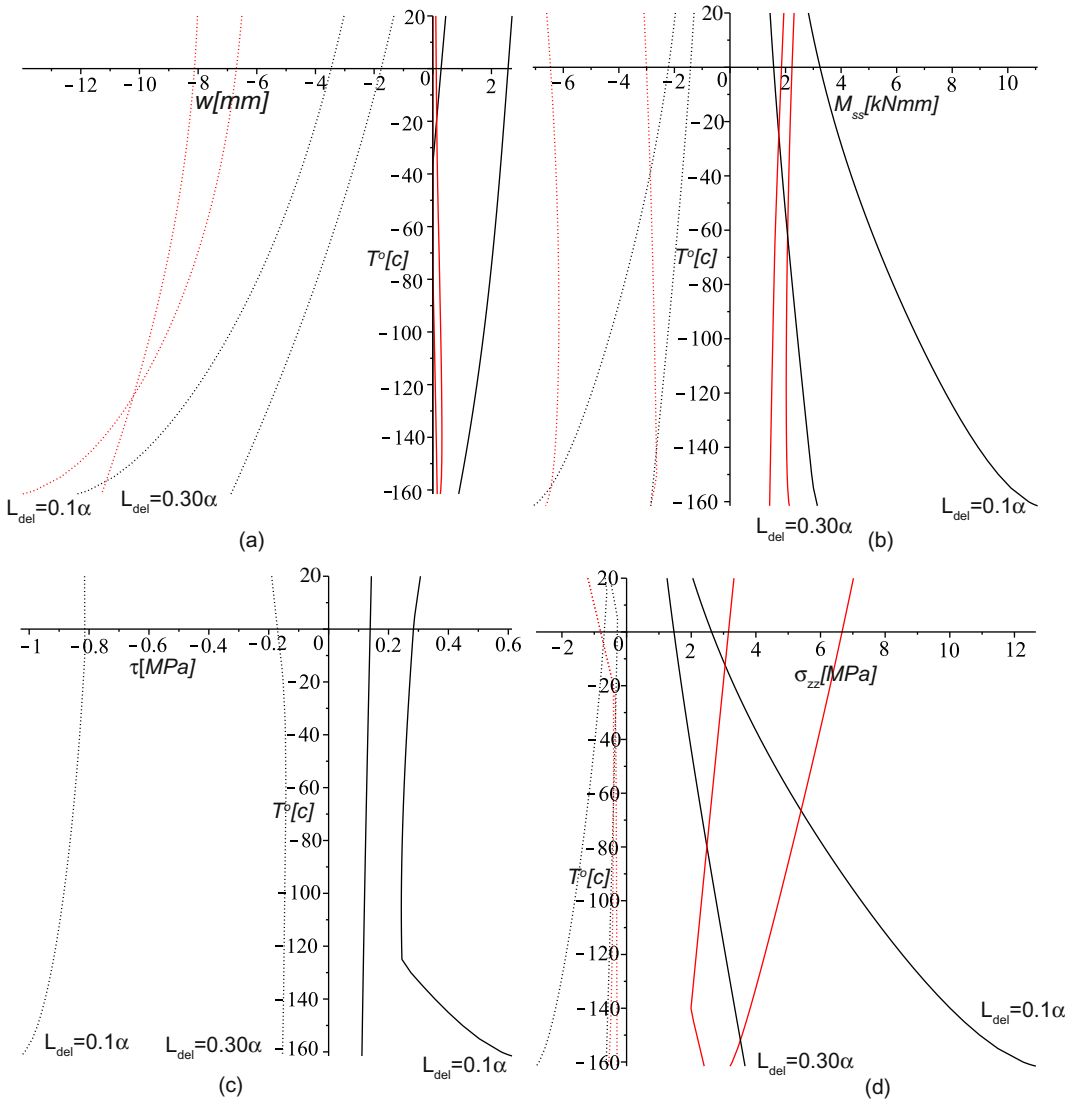

Fig. 16. Equilibrium curves for a debonded (L_{deb} = 0.10α, 0.30α) curved sandwich panel showing cooling temperature versus extreme structural values: at the face sheets: (a) radial displacements; (b) bending moment resultants; and in upper and lower face-core interfaces: (c) shear stresses; (d) radial normal stresses. Legend: black – upper face sheet, red — lower face sheet. (For interpretation of the references to colour in this figure legend, the reader is referred to the web version of this article.)

similar trends to those observed for the linear case, see Fig. 4, but with different displacement values. The ERR values and the extreme values of the interfacial shear and radial normal stresses at the crack tips, which appear in Fig. 9, are associated with non-convex behaviour that increases significantly as the crack/debond length increases. Notice that the curves for the ERR and lower interface radial normal stresses are quite similar, and that the predicted values are roughly an order of magnitude larger than predicted by the linear analysis, see Fig. 7.

The non-linear responses of a delaminated curved sandwich panel with a prescribed debond length and varying load appears in Figs. 10–12. The load has been applied through a radial displacement control of the lower face sheet at mid-span. The deformed shapes for various load levels, and with a debond length of 0.1α, appear in Fig. 10 from which is seen that the deformations increase with increasing load.

Fig. 11a to f describe the variation of some structural quantities along half of the sandwich panel circumference with a debonded region of 0.1α. Fig. 11a reveals that the radial displacements increase with increasing load. Moreover, it is seen that the displacements of the upper face sheet are smaller than the displacements of the lower face sheet,. The bending moment resultants, see Fig. 11b, display large values in the vicinity of the crack tips. The distributions of the circumferential face stress normal stress resultants, see Fig. 11c, reveal that at lower loads the reaction at the left support is in compression, but it changes to tension as the external load increases. It should be noticed that the stress resultants remain constants within the debonding region due to the absence of interfacial shear stresses. The circumferential displacements of the face sheets that appear in Fig. 11d are increasing in tandem with the loads. The interfacial shear (Fig. 7e) and radial normal stresses (Fig. 7f) reveal similar trends. Notice that they are extremely large at crack tips and null within the debonded region and they increase as the load increases.

Fig. 12 shows the equilibrium curves of load versus various extreme values of different load response quantities for debond lengths 0.1α and 0.3α, respectively. In all cases the response corresponds to that of an unstable structure with snap-through behaviour. The limit-point load becomes larger as the length of the debond crack decreases since the curved sandwich panel is stiffer when the debond crack length is smaller. The load versus radial displacement curves, see Fig. 12a, reveal that the limit point load is about 1.5 kN for a debond crack length of 0.1α, and it drops to about 0.3 kN for a length of 0.3α. The equilibrium curves for the

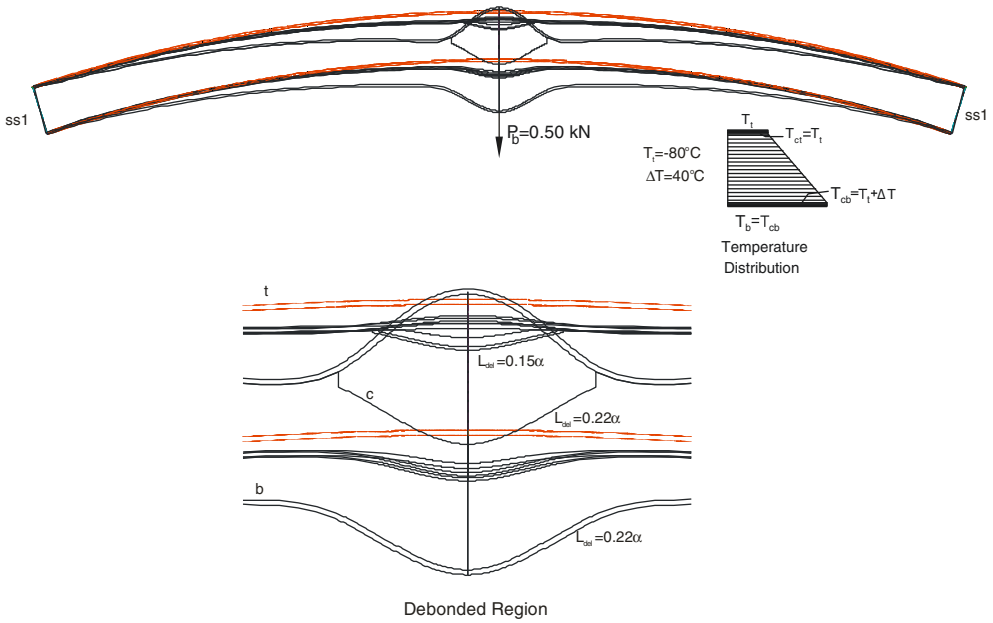

Fig. 17. Deformed shapes corresponding to a *non-linear* thermo-mechanical response of debonded curved sandwich panel for different debond lengths where $T_t = -80$ °C, $\Delta T = 40$ °C and $P_b = 0.5$ kN, and assuming *TI* mechanical properties: (a) overall shapes; (b) shapes in vicinity of debonded region.

bending moment resultant, see Fig. 12b, the circumferential displacements, see Fig. 12d, and the interfacial stresses, see Fig. 12e and f, display similar trends, but the actual curve patterns are somewhat more complex. The equilibrium curves for the circumferential normal stress resultants, see Fig. 12c, reveal a particularly complex response pattern.

3.1.2. Thermal loading only

The response of a debonded curved sandwich panel subjected to a uniform temperature distribution and with a core assumed to have temperature independent mechanical properties (*TI*) appears in Fig. 13. For this case the response is linear throughout the investigated range of temperatures from −200 to +200 °C. The deformed shapes corresponding to cooling from +20 to −200 °C, and heating from +20 to 200 °C, consist of almost a uniform inward and outward radial displacements around mid-span despite of the presence of a debonded zone in this region. It should be noticed that local bending occurs in the vicinity of the supports due to the imposed constraints that prevent the edges of the face sheets to move in the radial direction.

3.1.3. Thermo-mechanical loading

The thermo-mechanical response of a simply supported (*ss1* condition) curved sandwich panel subjected to a concentrated load applied at mid-span of lower face sheet, debond crack lengths of 0.1α and 0.3α, respectively, and with a temperature distribution that is uniform along the panel circumference, and with a gradient of 40 °C between the upper and the lower face sheets, appears in Figs. 14–16. The concentrated load is specified to 1.32 kN which corresponds to about 90% of the limit-point load when no thermal loading is applied, see Fig. 12. It is further assumed in this example that the mechanical properties of the core are unaffected by the temperature changes. The non-linear response is determined for varying temperatures of the upper face sheet.

For this case a non-linear thermo-mechanical response is detected only when cooling is applied (decreasing temperatures), i.e. the response remains linear when the temperature is increased. The deformed shapes for different lowered temperatures appear in Fig. 14, from which it is seen that the deformations increase with decreasing temperature values.

Fig. 15a to d describe the variation of various structural quantities along half the sandwich panel circumference for debond length of $L_{deb} = 0.1\alpha$. The radial displacements of the upper face sheet, see Fig. 15a, are associated with a deepening indentation in the lower face sheet, as the temperature level drops and the limit point temperature is reached, and an opposite indentation occurs at the upper debonded face sheet. This difference in the displacement between the two face sheets increases as the temperature is lowered. Significant bending moment resultants in the face sheets are observed in the vicinity of the external load and at the crack tips, see Fig. 15b. The values increase as the temperature is lowered and approaches the limit point temperature level. The interfacial shear stresses display high peak values at crack tips and zero values within the debonded region, see Fig. 15c. The radial interfacial stresses at the top and bottom face-core interfaces display extremely large tensile peak values at the crack tips, see Fig. 15d. It should be noticed that the stresses at the supports are quite small compared with the values encountered at the debond crack tips.

Fig. 16 shows the equilibrium curves of temperature versus various extreme values of different load response quantities for debond lengths of 0.1α and 0.3α, respectively. Fig. 16a describes the applied temperature versus the extreme values of the radial face sheet displacements, and it is seen that a limit point occurs at about −160 °C for the smaller delamination, where the solution stopped to converge, and that a slightly non-linear response is seen for the larger debond (0.3α). Similar trends are observed for the bending moment resultants, see Fig. 16b, the interfacial shear stresses, see Fig. 16c, and finally the radial normal stresses, see Fig. 16d.

The thermo-mechanical response at a temperature level of −80 °C, a thermal gradient of 40 °C between the top and bottom face sheets, and a concentrated load of 0.5 kN applied at mid-span of the lower face sheet is shown in Figs. 17 and 18 for debond crack lengths of 0.15α and 0.22α, respectively. The deformed shapes obtained for the 2 different debond crack lengths appear in Fig. 17. Results are presented up to a debond length of 0.22α only due to numerical difficulties. For the larger debond crack the upper face sheet moves upward significantly. The ERR values and the interfacial stresses at the crack tips appear in Fig. 18. The ERR (Fig. 18a) and maximum radial stress (Fig. 18c) values display non-convex

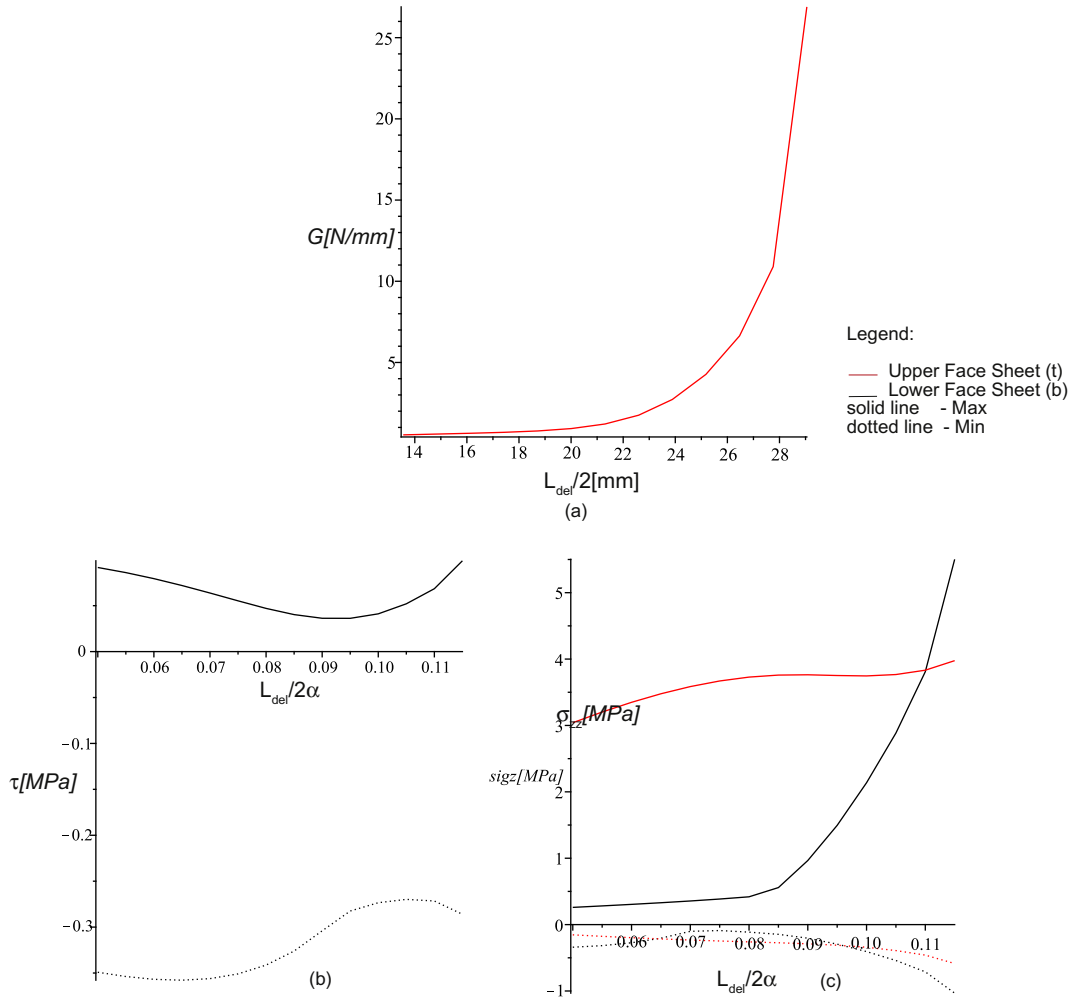

Fig. 18. Strain energy release rate (ERR) and extremum interfacial stresses corresponding to a *non-linear* thermo-mechanical response of a debonded curved sandwich panel where $T_t = -80$ °C, $\Delta T = 40$ °C and $P_b = 0.5$ kN, and assuming *TI* mechanical properties: (a) ERR; (b) interfacial shear stresses; (c) interfacial radial normal stresses. Legend: black – upper face sheet, red — lower face sheet, solid – maximum . . . – minimum. (For interpretation of the references to colour in this figure legend, the reader is referred to the web version of this article.)

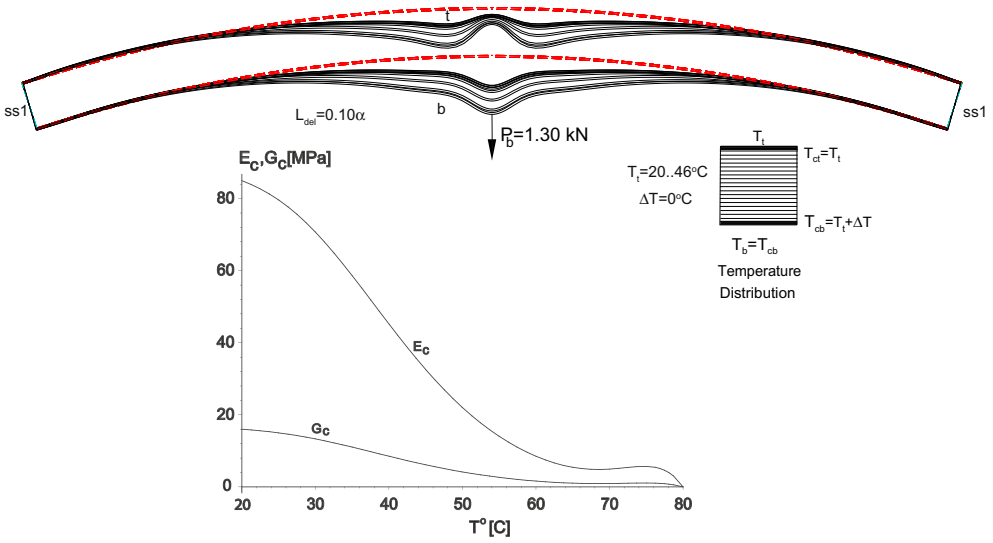

Fig. 19. Deformed shapes and temperature dependent (*TD*) core properties for non-linear thermo-mechanical response with $P_b = 1.3$ kN: (a) deformed shape and thermal distribution; (b) temperature dependence of elastic and shear moduli of core.

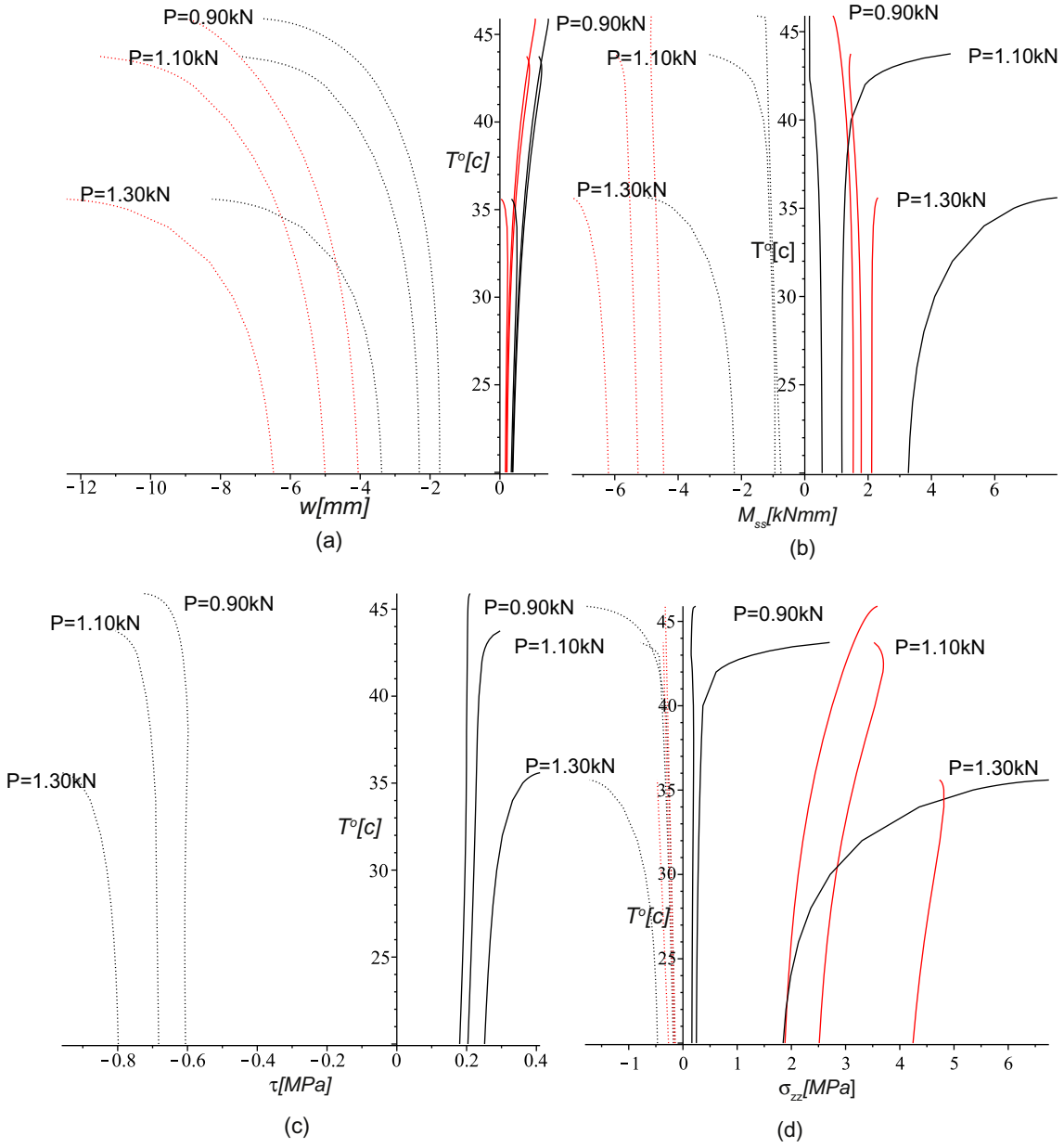

Fig. 20. Equilibrium curves of temperature (T_t) versus structural quantities for non-linear thermo-mechanical response of a debonded curved sandwich panel with *TD* properties, and a concentrated load applied at mid-span of the lower face sheet: In the face sheets: (a) radial displacements; (b) bending moment resultants; and at core-face interfaces: (c) shear stresses; (d) radial normal stresses. Legend: black – upper face sheet, red — lower face sheet. (For interpretation of the references to colour in this figure legend, the reader is referred to the web version of this article.)

curve patterns that increase with increasing length of the debond crack. The interfacial shear stresses, see Fig. 18b, are almost unaffected by the debond length. It should be noticed that these results resemble the results obtained for the purely mechanical load case, see Fig. 9. Hence, it can be concluded that the effects of temperature loading on the characteristic quantities of the debond region are insignificant for cooling temperatures that are above the limit point temperature level.

3.2. Temperature dependent mechanical properties

3.2.1. Thermo-mechanical loading

The thermo-mechanical response of a debonded sandwich panel, where it is assumed that the mechanical properties of the core properties are temperature dependent (*TD*), is presented in Figs. 19 and 20 for a debond crack length of 0.1α. The loading scheme from the previous example is adopted again, i.e. a concentrated load of 1.3 kN (about 90% of the limit point due to purely mechanical loading) is applied at mid-span, and the temperature distribution is assumed to be uniform through both the length and the depth of the sandwich panel.

The temperature-dependent (*TD*) core properties are specified according to the Divinycell HD grade PVC foam core data sheet of DIAB, (DIAB Divinycell, 2003), which includes measured material properties in a working range of temperatures between 20 and 80 °C. The temperature-dependent (*TD*) core material properties are defined through curve-fitting of the data that appears in the core material data sheet as follows, (DIAB Divinycell, 2003):

$$E_c(\phi, r_c) = E_{c0} f_T(T_c(\phi, r_c)), \quad G_c(\phi, r_c) = G_{c0} f_T(T_c(\phi, r_c))$$

with

$$f_T(T) = -2.82196349610^{-13}T^8 + 9.52831997110^{-11}T^7 + 0.03070734934^{T} - 1.32513499810^{-8}T^6 - 0.0095418123997T^2 + 9.70315767110^{-7}T^5 + 0.0008705288588T^3 - 0.000039522595147T^4 + 1.1903 \quad (22)$$

where E_{co} and G_{co} refer to the elasticity and shear moduli of the core at $T = 20$ °C. It should be noticed that if a thermal gradient is applied to the sandwich panel the mechanical properties of the core will also vary with the radial coordinate, see Fig. 19.

The deformed shape of the debonded curved sandwich panel is shown in Fig. 19 along with the variation of E_c and G_c with temperature. From Fig. 19 it is observed that both an indentation and a bulge at the upper face sheet occur, and that both of these tend to increase in amplitude with increasing temperature. It should be recognised that a pure thermal loading causes displacements in the upward direction, see Fig. 13, whereas the combined thermo-mechanical response yields large indentations at the lower face sheet as a result of the degradation of the core properties.

Fig. 20 shows the equilibrium curves of temperature versus various extreme values of different load response quantities for three different mechanical load values that are all below the limit point load level for pure mechanical loading, see Fig. 12, In all cases, a limit point behaviour is predicted, although with some numerical difficulties. The temperature versus the extreme radial displacement equilibrium curves appear in Fig. 20a. It shows that the temperature limit point level occurs at about 45° C for a load level of $P = 0.9$ kN, while the temperature limit temperature is about 43 °C for a load of $P = 1.1$ kN, and finally for a mechanical load 1.3 kN the critical temperature drops to around 35 °C. For all levels of mechanical loading the temperature limit point level is associated with a zero slope. The bending moment resultant equilibrium curves, see Fig. 20b, follow similar trends, but here the slope is not zero at the limit point temperature levels. Similar trends are observed for the interfacial shear stresses at the upper face-core interface, and the interfacial radial normal stresses, see Fig. 20c and d, respectively.

4. Summary and conclusions

The geometrically non-linear behaviour of a debonded curved sandwich panels subjected to thermal and mechanical loading with and without temperature dependent material properties is presented. The debond is assumed to exist at one of the face-core interfaces, and it is further assumed that the crack surfaces are free of shear tractions but can accommodate for the transfer of compressive contact stresses. The mathematical formulation presents the governing field equations along with the appropriate boundary and continuity conditions of debonded regions with and without contact. The mathematical formulation is based on a variational approach that follows the high-order sandwich panel theory (HSAPT) computational model. Thermal straining of the core along with the effects of radial (through thickness) core flexibility within the fully bonded and debonded regions is considered. The core stress and the displacement fields within the debonded region are determined explicitly, with and without contact, and for the case of a core with temperature independent (*TI*) or temperature dependent (*TD*) mechanical properties. An explicit description of the non-linear governing equations of the debonded region is presented for the *TI* case. The stress and the displacements fields of the debonded core regions, with and without contact, in the case of Temperature Dependent (*TD*) properties are determined by a closed-form solution using a polynomial description for the distribution of the mechanical properties through the thickness of the core. The non-linear response is determined through the solution of the non-linear governing equations of the various regions along with the appropriate boundary and continuity conditions using a finite-differences scheme along with a natural parametric continuation and a pseudo arc-length procedure.

The numerical study investigates the non-linear response of delaminated curved sandwich panels subjected to mechanical concentrated loads, thermally induced deformations and simultaneous thermal and mechanical loads. The imposed mechanical loads are below the limit point load level of the mechanical response, and the imposed temperature field is varied in the modelling. The modelling results are displayed in terms of plots of various structural quantities along the sandwich panel length (circumference), equilibrium curves and strain energy release rate curves. It is shown that the thermo-mechanical response shifts the linear or non-linear responses, observed for the separate cases of either temperature induced deformations or mechanical loading, into a strongly non-linear response with limit point behaviour and associated stability problems.

The proposed computational models based on the HSAPT approach enhance the physical insight of the thermo-mechanical response of debonded curved sandwich panels. Thus, the numerical study has revealed the general occurrence of limit-point behaviour due to both purely mechanical and combined thermal and mechanical loads, whereas the response due to purely thermal loading remains linear. The degradation of the core properties with increasing temperature yields limit-point behaviours that are unstable at quite low temperatures, and well within the working range of temperatures for Divinycell HD grade PVC foam core materials. Hence, the existence of debonds/delaminations together with thermally induced deformations and mechanical loading in curved sandwich panels is a combination that should be avoided. Accordingly, it is suggested that precaution measures should be taken to detect such imperfections to ensure the structural integrity, and there by enable the safe operation of curved sandwich panels exposed to combined thermal and mechanical loadings.

Acknowledgement

The work presented was sponsored by the US Navy, Office of Naval Research (ONR), Award N000140710227, "Influence of local effects in sandwich structures under general loading conditions and ballistic impact on advanced composite and sandwich structures", and the Ashtrom Engineering Company that supports the professorship chair of Prof. Frostig. The ONR program manager was Dr. Yapa D.S. Rajapakse. The financial support received is gratefully acknowledged.

References

Allen, H.G., 1969. Analysis and Design of Structural Sandwich Panels. Pergamon Press, Oxford.

Ascher, U.M., Petzold, L., 1998. Computer Methods for Ordinary Differential Equations and Differential-Algebraic Equations. SIAM, Philadelphia.

Avery, J.L., Manickam, N., Sankar, B.V., 1998. Compressive failure of debonded sandwich beams. In: Sankar, B.V. (Ed.), Recent Advances in Mechanics of Aerospace Structures and Materials, Proceedings of ASME International Mechanical Engineering Congress and Exposition, AD-vol. 56. ASME, New York, pp. 207–217.

Avile's, F., Carlsson, L.A., 2005. Elastic foundation analysis of local face buckling in debonded sandwich columns. Mechanics of Materials 37, 1026–1034.

Avile's, F., Carlsson, L.A., 2008. Analysis of the sandwich DCB specimen for debond characterization. Engineering Fracture Mechanics 75, 153–168.

Bozhevolnaya, E., 1998. A Theoretical and Experimental Study of Shallow Sandwich Panels, Ph.D. Thesis, Institute of Mechanical Engineering, Aalborg University, Denmark.

Bozhevolnaya, E., Frostig, Y., 1997a. Nonlinear Closed-Form High-Order Analysis of Curved Sandwich Panels. Composite Structures 38 (1–4), 383–394.

Bozhevolnaya, E., Frostig, Y., 1997b. Nonlinear closed-form high-order analysis of curved sandwich panels. Composite Structures 38 (1-4), 383–394.
Bozhevolnaya, E., Frostig, Y., 2001. Free vibration of curved sandwich beams with a transversely flexible core. Journal of Sandwich Structures and Materials 3 (4), 311–342.
Char, B.W., Gedddes, K.O., Gonnet, G.H., Leong, B.L., Monagan, M.B., Watt, S.M., 1991. Maple V Library Reference Manual. Springer-Verlag, New-York.
DIAB Divinycell, 2003. Data Sheet for DivinycellHD Grade PVC foams. Diab Group, Sweden.
Di Sciuva, M., Carrera, E., 1990. Static buckling of moderately thick, anisotropic, laminated and sandwich cylindrical shell panels. AIAA Journal 28 (10), 1783–1793.
Frostig, Y., 1992. Behavior of delaminated sandwich beams with transversely flexible core - high order theory. Composite Structures Journal 20, 1–16.
Frostig, Y., 1999. Bending of curved sandwich panels with transversely flexible cores – closed-form high-order theory. Journal of Sandwich Structures & Materials 1, 4–41.
Frostig, Y., Sokolinsky, V., 2000. High-order buckling of debonded (delaminated) sandwich panels with a soft core. AIAA Journal 38 (11), 2147–2159.
Frostig, Y., Thomsen, O.T., 2005. Non-linear behavior of delaminated sandwich panels with partial contact and a transversely flexible core. International Journal of Non-Linear Mechanics 40 (5), 633–651.
Frostig, Y., Thomsen, O.T., 2007. Buckling and non-linear response of sandwich panels with a compliant core and temperature-dependent mechanical properties. Journal of Mechanics of Materials and Structures 2 (7), 1355–1380.
Frostig, Y., Thomsen, O.T., 2008. Title thermal buckling and postbuckling of sandwich panels with a transversely flexible core. AIAA Journal 46 (8), 1976–1989.
Frostig Y., Thomsen O.T., 2009. Non-linear behavior of thermally heated curved sandwich panels with a transversely flexible core. Journal of Mechanics of Materials and Structures.
Frostig, Y., Baruch, M., Vilnai, O., Sheinman, I., 1992. High-order theory for sandwich-beam bending with transversely flexible core. Journal of ASCE, EM Division 118 (5), 1026–1043.
Frostig, Y., Thomsen, O.T., Vinson, J.R., 2004. High-order bending analysis of unidirectional curved soft sandwich panels with disbonds and slipping layers. Journal of Sandwich Structures & Materials 6 (2), 167–194.
Hildebrand, M., 1991. On the bending and transverse shearing behavior of curved sandwich panels. Technical Research center of Finland, RN 1249.
Hwu, C., Hu, J.S., 1992. Buckling and postbuckling of delaminated composite sandwich beams. AIAA Journal 30 (7), 1901–1909.
Kant, T., Kommineni, J.R., 1992. Geometrically non-linear analysis of doubly curved laminated and sandwich fiber reinforced composite shells with a higher order theory and C^0 finite elements. Journal of Reinforced Plastics and Composite Materials 11 (19), 1048–1076.
Kardomateas, G.A., 1998. Growth of face-sheet delaminations in sandwich beams under compression or bending. In: Sankar, B.V. (Ed.), Recent Advances in Mechanics of Aerospace Structures and Materials, Proceedings of the ASME International Mechanical Engineering Congress and Exposition, AD-vol. 56. ASME, New York, pp. 173–180.
Karyadi, E., 1998. Collapse behavior of imperfect sandwich cylindrical shells. Ph.D. Thesis. Delft University of Technology, Faculty of Aerospace Engineering, The Netherlands.
Keller, H.B., 1992. Numerical Methods for Two-Point Boundary Value Problems. Dover Publications, New York.
Kuhhorn, A., Schoop, H., 1992. A nonlinear theory for sandwich shells including the wrinkling phenomena. Archive Applied Mechanics 62, 413–427.
Librescu, L., Hause, T., 2000. Recent developments in the modeling and behavior of advanced sandwich constructions: a survey. Composite Structures 48 (1), 1–17.
Librescu, L., Lin, W., Nemeth, M.P., Starnes, J.H., 1994. Effects of tangential edge constraints on the post-buckling behavior of flat and curved panels subjected to thermal and mechanical loads. In: Buckling and Postbuckling of Composite Structures. Proceedings of the International Mechanical Engineering Congress, November 6–11, Chicago, USA, vol. 41, pp. 55–71.
Librescu, L., Nemeth, M.P., Starnes Jr., J.H., Lin, W., 2000. Nonlinear response of flat and curved panels subjected to thermomechanical loads. Journal of Thermal Stresses 23, 549–582.
Lin, C.C., Cheng, S.H., Wang, J.T.S., 1996. Local buckling of delaminated composite sandwich plates. AIAA Journal 34 (10), 2176–2183.
Lyckegaard, A., Thomsen, O.T., 2004. High order analysis of junction between straight and curved sandwich panels. Journal of Sandwich Structures and Materials 6 (November), 497–525.
Lyckegaard, A., Thomsen, O.T., 2006. Nonlinear analysis of a curved sandwich beam joined with a straight sandwich beam. Composites Part B: Engineering 37 (2-3), 101–107.
Noor, A.K., Burton, W.S., Bert, C.W., 1996. Computational models for sandwich panels and shells. Applied Mechanics Review 49, 155–199.
Plantema, F.J., 1966. Sandwich Construction. John Wiley & Sons, New York.
Rabinovitch, O., Frostig, Y., 2002. High-order behavior of fully and partially bonded (delaminated) circular sandwich plates with generally laminated face sheets and a soft core. International Journal of Solids and Structures 39 (11), 3057–3077.
Rao, K.M., Meyer-Piening, H.R., 1990. Buckling analysis of FRP faced cylindrical sandwich panel under combined loading. Composite Structures 14, 15–34.
Schwarts-Givli, H., Rabinovitch, O., Frostig, Y., 2007. High order nonlinear contact effects in the dynamic behavior of delaminated sandwich panels with flexible core. International Journal of Solids and Structures 44 (1), 77–99.
Simitses, G.J., Sallam, S., Yin, W.L., 1985. Effect of delamination of axially loaded homogeneous laminated plates. AIAA Journal 23 (9), 1437–1444.
Smidt, S., 1995. Bending of curved sandwich beams. Composite Structures 33, 211–225.
Somers, M., Weller, T., Abramovich, H., 1991. Influence of predetermined delaminations on buckling and postbuckling behavior of composite sandwich beams. Composite Structures 17 (4), 295–329.
Sridharan, S., Li, Y., 2006. Static and dynamic delamination of foamcore sandwich members. AIAA JOURNAL 44 (12), 2937–2948.
Stoer, J., Bulirsch, R., 1980. Introduction to Numerical Analysis. Springer, New York.
Thomsen, O.T., Vinson, J.R., 2001. Analysis and parametric study of non-circular pressurized sandwich fuselage cross section using high-order sandwich theory formulation. Journal of Sandwich Structures and Materials 3 (3).
Tolf, G., 1983. Stresses in a curved laminated beam. Fibers Science and Technology 19 (4), 243–267.
Vaswani, J., Asnani, N.T., Nakra, B.C., 1988. Vibration and damping analysis of curved sandwich beams with a viscoelastic core. Composite Structures 10 (3), 231–245.
Vinson, J.R., 1999. The Behavior of Sandwich Structures of Isotropic and Composite Materials. Technomic Publishing Co. Inc., Lancaster.
Zenkert, D., 1991. Strength of sandwich beams with interface debondings. Composite Structures 17 (4), 331–350.
Zenkert, D., 1995. An Introduction to Sandwich Construction. Chameleon Press Ltd, London.